Modified desolvation method enables simple one-step synthesis of gelatin nanoparticles from different gelatin types with any bloom values

Pavel Khramtsov[1,2,3], Oksana Burdina[2], Sergey Lazarev[2], Anastasia Novokshonova[2], Maria Bochkova[1,2], Valeria Timganova[1], Dmitriy Kiselkov[4], Svetlana Zamorina[1,2], Mikhail Rayev[1,2]*

[1]Institute of Ecology and Genetics of Microorganisms, Perm Federal Research Center of the Ural Branch of the Russian Academy of Sciences, 614081, 13 Golev st., Perm, Russia

[2]Department of Biology, Perm State University, 614068, 15 Bukirev st., Perm, Russia

[3]Center for Immunology and Cellular Biotechnology, Immanuel Kant Baltic Federal University, 236016, 14 A. Nevski st., Kaliningrad, Russia

[4]Institute of Technical Chemistry, Perm Federal Research Center of the Ural Branch of the Russian Academy of Sciences, 614013, 3 Academician Korolev st., Perm, Russia

**Corresponding author: e-mail: khramtsovpavel@yandex.ru, phone: +7 (342) 2807794, 614081, 13 Golev st., Perm, Russia*

Graphical abstract

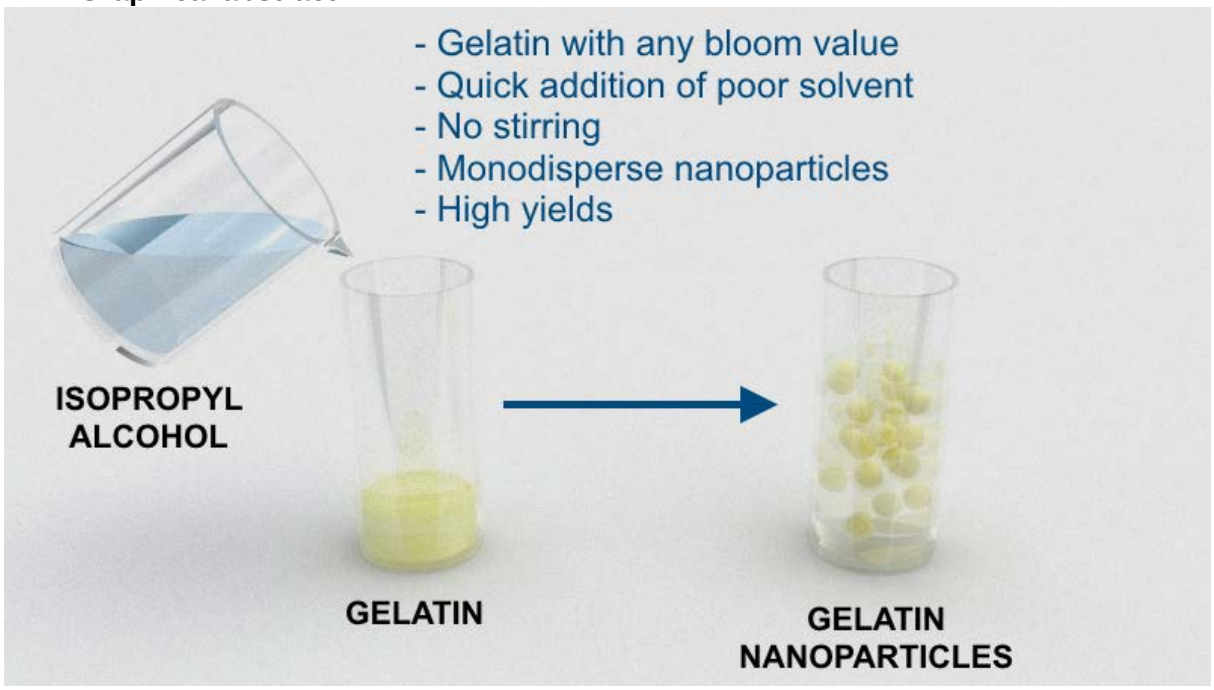

Abstract

Gelatin nanoparticles found numerous applications in drug delivery, bioimaging, immunotherapy, and vaccine development as well as in biotechnology and food science. Synthesis of gelatin nanoparticles is usually made by a two-step desolvation method, which, despite providing stable and homogeneous nanoparticles, has many limitations, namely complex procedure, low yields, and poor reproducibility of the first desolvation step. Herein, we present a modified one-step desolvation method, which enables the quick, simple, and reproducible synthesis of gelatin nanoparticles. Using the proposed method one can prepare gelatin nanoparticles from any type of gelatin with any bloom number, even with the lowest ones, which remains unattainable for the traditional two-step technique. The method relies on quick one-time addition of poor solvent (preferably isopropyl alcohol) to gelatin solution in the absence of stirring. We applied the modified desolvation method to synthesize nanoparticles from porcine, bovine, and fish with bloom values from 62 to 225 on the hundreds-of-milligram scale. Synthesized nanoparticles had average diameters between 130 and 190 nm and narrow size distribution. Yields of synthesis were 62-82% and can be further increased. Gelatin nanoparticles have good colloidal stability and withstand autoclaving. Moreover, they were non-toxic to human immune cells.

Keywords
Gelatin, nanoparticles, desolvation, manufacturing, yield, nanocarriers, drug delivery

1. Introduction

Gelatin is a product of partial hydrolysis of collagen. In the course of gelatin preparation, collagen is pre-treated under acidic or alkaline conditions, which results in obtaining two types of gelatin: type A and type B respectively. The main sources of gelatin are bovine skin, bovine hides, and cattle and pork bones, whereas fish and poultry gelatines are used to a limited extent (**Gomez-Guillen, 2011**). Gelatin from cold-water fish contains a lower percentage of proline and hydroxyproline which are involved in the formation of collagen-like triple helices and therefore has inferior gelation properties in comparison with mammalian gelatins (**Gomez-Guillen, 2011, Derkach, 2020**). Being biocompatible (included in FDA's GRAS list), low-immunogenic, cheap, and commonly available biopolymer gelatin gains popularity in biomedicine, biotechnology, and food science (**Khan, 2020**). Conditions in which hydrolysis of collagen is performed affect the size distribution of resulting gelatin molecules. Size distribution of gelatin molecules usually correlates with gel strength which is expressed as a Bloom value: the longer gelatin polypeptide chains the higher gel strength and Bloom value (**Alipal, 2021**).

Gelatin, as well as many other proteins, is used in the form of gelatin nanoparticles. Drug delivery is arguably the scientific field most intensively taking advantage of gelatin nanoparticles. Indeed, many reports of gelatin-based nanotherapeutics and nanovaccines were made in the past years. Below some representative examples of successful *in vivo* applications of gelatin nanoparticles-based nanomedicines are presented.

Application of gelatin nanoparticles allowed the same therapeutic effect with the five-fold lower dose of timolol maleate for glaucoma treatment on mice model in comparison with conventional therapy (free timolol maleate) (**Esteban-Pérez, 2020**). Gelatin nanoparticles and their aminated counterparts exhibited immunomodulatory efficiency comparable to that of aluminum adjuvants being non-immunogenic by themselves (**Sudheesh, 2010**). Pegylated gelatin nanoparticles showed excellent biocompatibility and significantly improved release kinetics and bioavailability of ibuprofen after parenteral administration (**Narayanan, 2013**). Gelatin nanoparticles loaded with immunostimulatory cytosine-phosphate-guanosine oligodeoxynucleotides provided long-term positive effects in horses with asthma and showed higher efficacy in comparison with standard therapy (**Klier, 2019**). Antimicrobial gelatin nanoparticles modified with selenium nanoparticles and ruthenium complexes and coated with erythrocyte membranes were tested *in vivo* on mice. Nanoparticles accumulated in the injury site and provided elimination of methicillin-resistant *Staphylococcus aureus*, their efficiency was equal to that of vancomycin (**Lin, 2019**).

Potential applications of gelatin nanoparticles are not limited to therapeutics and vaccine development. Gelatin nanoparticles and microparticles together with molecular gelatin can serve as cheap collagen substitutes imitating extracellular matrix in cell culturing and tissue engineering (**Bello, 2020**). Gelatin nanoparticles improve the mechanical properties (induction of thixotropy) of bioinks for 3D bioprinting (**Clark, 2019, Diba, 2021)** and increased circulating tumor cell capture in a microfluidic device **(Wei, 2019).** Preparation of Pickering emulsions for food chemistry is another prominent application of gelatin nanoparticles (**Feng, 2020**).

Desolvation is one of the most popular techniques for gelatin nanoparticle synthesis (**Khan, 2020**). Desolvation relies on the addition of poor solvents (usually acetone, alcohols, or acetonitrile) to the aqueous protein solution. Desolvation of gelatin is regularly performed in two steps according to the method described by Coester et al. (**Coester, 2000**) and further optimized by researchers from the same scientific group (**Zwiorek, 2006, Ahlers, 2007**). The first step of desolvation includes the addition of non-solvent to gelatin solution resulting in sedimentation of high-molecular gelatin fractions. Sediment is dissolved in water, then, after the pH adjustment, repeated addition of non-solvent results in the formation of gelatin nanoparticles. Being a relatively simple and accessible method of synthesis of stable and biocompatible gelatin nanoparticles, two-step desolvation is widely used in various fields. Shortcomings of two-step desolvation are low particle yields, lack of reproducibility of the first desolvation step, and difficult process scale-up (**Geh, 2016**). Therefore, numerous efforts were made to develop a more straightforward, one-

step technique. It has been shown that the presence of low-molecular-weight fractions (more than 20% of fractions with molecular weight less than 65 kDa) in gelatin preparations leads to the formation of non-stable and polydisperse nanoparticles. These very fractions need to be removed with the first desolvation step (**Zwiorek, 2006, Ahlers, 2007)**.

Several approaches were proposed to prepare gelatin nanoparticles by the desolvation method in one step. The first approach is to use custom-made or recombinant gelatin lacking low-molecular-weight fractions (**Ahlers, 2007, Won, 2008).** The disadvantage of this method is limited availability and the high cost of starting material. Commercially available high-bloom gelatin (bloom value of 300) allows to skip the first desolvation step (**Geh, 2016**), however resulting nanoparticles tend to aggregate (**Madkhali, 2018**). Vacuum filtration was used to get rid of large molecular weight gelatin and increase the homogeneity of gelatin before desolvation (**Stevenson, 2018**). Shamarekh et al. prepared gelatin enriched with high-molecular-weight fractions from commercial gelatin and used it as a starting material (**Shamarekh, 2020**). Despite these last two methods allowing desolvation to be made in one step, they are rather quasi-one-step than true one-step because both of them still require depletion of smaller gelatin molecules.

Surprisingly, several research groups reported the synthesis of uniform gelatin nanoparticles by one-step desolvation without removal of low-molecular-weight fractions (**Kaul, 2002, Kommareddy, 2008, Ofokansi, 2010, Esteban-Pérez, 2020**). All these groups used gelatin with bloom 225 or lower, which is expected to be not compatible with the one-step method. Most of these works lack an explanation of why proposed synthesis protocols are effective, however, Ofokansi et al. claimed that neutral pH facilitated stability and homogeneity of nanoparticles (**Ofokansi, 2010**).

We revealed that the stirring speed of the gelatin solution dramatically influences the desolvation process. Intensive stirring promotes gelatin aggregation. Using a simple one-step stirring-free approach we previously prepared stable and homogeneous gelatin nanoparticles from gelatin with bloom value as low as 75 (**Khramtsov, 2021**). Based on these findings we intended to develop a facile method for nanoparticle preparation from any type of gelatin with any bloom number. Hence, the goals of this work were as follows:

1. To confirm the effect of stirring on desolvation of gelatin;
2. To study the influence of gelatin pH, concentration, and non-solvent type on the size and yield of gelatin nanoparticles;
3. Using optimized conditions to synthesize nanoparticles from porcine, bovine, and fish gelatin with different bloom values (including lowest values available) in a hundreds-of-microgram scale;
4. To study storage stability and colloidal stability of resulting nanoparticles;
5. To load model hydrophobic molecule into gelatin nanoparticles;
6. To assess the effect of sterilization on the integrity of gelatin nanoparticles;
7. To study cytotoxicity of gelatin nanoparticles prepared by modified desolvation method.

2. Materials and methods

2.1. Materials

Gelatin B, 75 bloom (lot# G6650); gelatin B, 225 bloom (lot# G9382); cold water fish gelatin (lot# G7041), gelatin A, 62 bloom (lot# 48720); gelatin A, 180 bloom (lot# 48722) BCA assay kit, 1,10-phenanthroline, and boric acid were obtained from Sigma Aldrich (USA). Glutaraldehyde (50%) was obtained from ITW Reagents (USA). Trypsin was obtained from Samson-Med (Russia). Diacoll was obtained from Dia-M (Russia). Propidium iodide was obtained from eBioscience (USA). DMSO was obtained from Tula Pharmaceutical Plant (Russia). Water for injections was obtained from Solopharm (Russia). Sodium hydroxide, sodium chloride, sodium hydrogen phosphate, sodium dihydrogen phosphate, sodium bicarbonate, sodium hydrocarbonate, glycine were obtained from ITW Reagents (USA). Isopropyl alcohol, ethanol, methanol, hydrochloric acid, acetic acid were obtained from Vekton (Russia).

4-(4-methylphenyl)-2,4-dioxobutanoic acid was obtained from commercially available reagents by the Claisen condensation (**Beyer, 1887**) and kindly provided by Ekaterina Khramtsova, department of Organic Chemistry, PSU.

The following instrumentation was used: peristaltic pump, LKB (Sweden), Synergy H1 plate reader, BioTek (USA), Multiskan Sky UV-Vis Reader, Thermo (USA) and ZetaSizer NanoZS

particle analyzer, Malvern (UK), CytoFLEX flow cytometer, Beckman Coulter (USA), SV-10 viscometer, A&D (Japan). Multipette M4, Eppendorf (Germany) was used for accurate dispensing of viscous gelatin solutions.

2.2. Preparation of gelatin stock solutions

Gelatin powder was added to a certain volume of water and incubated at +40 °C until a clear solution was obtained. Gelatin solution was aliquoted and stored at +4 °C. The concentration of gelatin was determined gravimetrically as follows. Gelatin solution (1 ml) was added to the porcelain crucible and dried to constant weight at subsequently +95 °C and +140 °C. Three replicates were done for each sample. The concentration of gelatin nanoparticles was measured in the same way.

2.3. Optimization experiments

2.3.1. Preliminary assessment of factors affecting size and yield of gelatin nanoparticles: small-scale syntheses with gelatin B 75 bloom.

In 2 ml centrifuge tubes 200 µl of gelatin solution was added. Tubes were kept in a dry-block thermostat at +37 °C. Ethanol (96%), methanol (99,8%), and isopropyl alcohol (99,8%) were prewarmed in the water bath at +37 °C. Alcohol was added to the gelatin solution, then mixed for 5 min on a rotator mixer (10 rpm, 360 degrees), and kept in the thermostat at +37 °C for 30 min. 45 µl of 0,8% glutaraldehyde solution was added to each tube, mixed, and left in the thermostat as described above. Unreacted glutaraldehyde was quenched by adding 100 µl of 1 M glycine. Tubes were mixed and kept in the thermostat for 60 min (glycine addition was omitted for samples with initial gelatin concentrations of 2% and 4% due to partial nanoparticle aggregation). Cross-linked nanoparticles were centrifuged at 10000 g and washed with water 4 times. After each centrifugation cycle nanoparticles were redispersed by sonication (10 s, 60% amplification, 3 mm probe, approx. 8 W). Purified nanoparticles were stored at +4 °C. The size of nanoparticles was measured immediately after the preparation. The concentration of gelatin was determined when all the samples were synthesized. The storage period of individual bathes varied from 1 week to 2 months. Before protein quantification nanoparticles were sonicated to obtain homogeneous suspension (10 s, 60% amplification, 3 mm probe, approx. 8 W).

In the course of the experiment, we varied the pH of gelatin solution (pH values were 8, 9, and 10), the concentration of gelatin (8, 16, and 32 mg/ml), and the volume of added alcohol (600 and 1000 µl).

2.3.2. Optimization of gelatin nanoparticles preparation: gelatin B, 75 bloom, gelatin B, 225 bloom, fish gelatin, gelatin A, 62 bloom, gelatin A, 180 bloom.

Ethanol (96%), isopropyl alcohol (99,8%), and gelatin solutions were prewarmed in the water bath at +37 °C. In 50 ml centrifuge tubes containing 4 ml of gelatin solution, a certain volume of ethanol or isopropyl alcohol was added. Tubes were briefly and gently mixed on a rotating mixer (360 degrees, 10 rpm, 5 rounds) and kept in a thermostat at +37 °C for 30 min. Nine hundred microliters of 0,8% glutaraldehyde solution were added to each tube, which was gently mixed (as in the previous step), and left in the thermostat for another 30 min. Cross-linked nanoparticles were transferred to 85 ml polycarbonate centrifuge tubes and centrifuged at 15000 g for 60 min. Sediment was redispersed in the 2 ml of deionized water (when the amount of nanoparticles was too high they were redispersed in 4 ml of water) using sonication and pipette-assisted mixing. Concentrated suspension of gelatin nanoparticles was quantitatively transferred into 2 ml centrifuge tubes (1 ml of nanoparticle suspension per tube) and centrifuged two times at 20000 g for 30 min. After each centrifugation cycle, the supernatant was removed, and nanoparticles were redispersed in 900 or 1000 µl of deionized water (volume of water was decreased when pellet was large) by sonication (10 s, 60% amplification, 3 mm probe, approx. 8 W). Purified nanoparticles were stored at +4 °C. The size of nanoparticles was measured immediately after the preparation. The concentration of gelatin was determined when all the samples were synthesized. The storage period of individual bathes varied from 1 week to 3 months. Before protein quantification nanoparticles were sonicated to obtain homogeneous suspension (10 s, 60% amplification, 3 mm probe, approx. 8 W).

In the course of the experiment, we varied the pH of gelatin solution (pH values were 9 and 10), the concentration of gelatin (5, 9, and 18 mg/ml), and the volume of added alcohol (12, 20, and 28 ml). The pH of the gelatin solution was adjusted by 1 M NaOH, which volume was

negligible in relation to the volume of gelatin and, therefore, did not affect the final concentration of gelatin.

Determination of nanoparticle yield. Nanoparticles were homogenized by brief sonication and diluted in phosphate buffer, pH 7. Trypsin was added to the final concentration of 10 μg/ml. Samples were incubated at +37 °C in the thermostat until the solution became clear (OD values at 600 nm as low as in nanoparticle-free samples). Gelatin calibrators were treated in the same way. Twenty-five microliters of digested samples were transferred to a 96-well plate; then 200 μl of BCA reagent was added, and the resulting mixture was incubated for 30 min at +37 °C in the plate thermostat (400 rpm). Absorbance was measured at 562 nm.

Size of nanoparticles was determined by the DLS technique. For DLS measurements nanoparticles were diluted at 1:375 in water. Hereinafter z-average hydrodynamic diameters are given.

2.4. Synthesis of gelatin nanoparticles in hundred-of-milligram scale

Gelatin A (bloom 62 and 180), gelatin B (bloom 75 and 225), and fish gelatin were diluted in water to 10 mg/ml, then pH was adjusted to 10 (to 11 for gelatin A and fish gelatin) with 1 M NaOH. One hundred milliliters of the resulting solution was desolvated by 500 ml of isopropyl alcohol, and the mixture was incubated for 30 min at +37 °C in the water bath. Gelatin solutions and isopropyl alcohol were kept in the water bath at +37 °C prior to mixing. Then, 22.5 ml of 0.8% glutaraldehyde was quickly added, followed by 30-min-long incubation at +37 °C in the water bath. Cross-linked nanoparticles were transferred into polycarbonate 85 ml centrifuge tubes and centrifuged at 15000 g for 60 min. Pellets were combined and redispersed in 60 ml of water with sonication (10-30 s, 60% amplification, 3 mm probe, approx. 8 W), resulting suspensions were centrifuged at 15000 g for 30 min two more times. After the final centrifugation, 40 ml of water was added to the pellet, and the resulting suspension was sonicated for 20 min (60% amplification, 6 mm probe, approx. 25 W) on ice. The concentration of nanoparticles was determined by gravimetric analysis.

For fluorescence measurements samples were diluted to 1 mg/ml with water; then 100 μl of each sample was transferred into the wells of black 96-well plates. In order to obtain SEM images, nanoparticles were diluted in water to 1 μg/ml, dropped at 5x5 mm silicon wafer, and dried overnight at room temperature. For SEM experiments glycine-quenched nanoparticles were taken to reduce the possibility of interaction between free aldehyde groups and amine groups located on the nanoparticles' surface in the course of drying.

2.5. Preparation of gelatin nanoparticles loaded with fluorescent europium chelates

Gelatin A (bloom 62 and 180), gelatin B (bloom 75 and 225), and fish gelatin were diluted in water to 10 mg/ml then pH was adjusted to 10 (to 11 for gelatin A and fish gelatin) with 1 M NaOH. Four milliliters of the resulting solution was desolvated by 20 ml of ethanol containing 4-(4-Methylphenyl)-2,4-dioxobutanoic acid, 1,10-phenanthroline, and europium chloride (concentrations were 180 μM, 60 μM, and 60 μM respectively), and the mixture was incubated for 30 min at +37 °C in the thermostat (**Mironov, 2017**). Solutions containing gelatin and fluorescent complexes were kept on the water bath at +37 °C before mixing. Then, 900 μl of 0.8% glutaraldehyde was added, followed by 30-min-long incubation at +37 °C. Nanoparticles were transferred into polycarbonate 85 ml centrifuge tubes and centrifuged at 15000 g for 60 min. Pellet was redispersed in 4 ml of water with sonication and centrifuged three times at 20000 g for 30 min. After each wash pellet was redispersed in water by sonication (10-30 s, 60% amplification, 3 mm probe, approx. 8 W). Supernatants obtained after the final washing step were collected. For fluorescence measurements tenfold dilutions of nanoparticles in water were prepared; then 100 μl of each dilution was transferred into the wells of black 96-well plates.

2.6. Steam autoclaving

Glycine quenching. Before sterilization 1 M glycine-NaOH buffer pH 9.3 was added to gelatin nanoparticles suspension (1 part of buffer per 9 parts of suspension) resulting mixture was incubated for 1 h at +37 °C on a rotator (10 rpm, 360 degrees). Nanoparticles were then washed three times with water by centrifugation at 15000 g for 1 h. The concentration of nanoparticles was determined by gravimetric analysis.

Autoclaving. Five milliliters of the resulting nanoparticle suspension were placed in the 15 ml amber glass vials and autoclaved for 15 min at 0.5 atm above atmospheric pressure. Suspensions were cooled at room temperature and stored at +4 °C. Control nanoparticles were kept at +4 °C.

Removal of nanoparticle aggregates after autoclaving. 1 ml of nanoparticle suspension was moved to centrifuge tubes. Nanoparticles were centrifuged at 1000 g for 10 min. After centrifugation nanoparticle size was measured by DLS. Triple replicates were performed for each measurement.

Characterization. The optical density of nanoparticle suspensions was measured before and after centrifugation. The suspension was diluted in distilled water. The measurement was performed at 600 nm. For DLS measurements nanoparticles were diluted at 1:375 in PBS (pH 7). Zeta potential of autoclaved nanoparticles was measured at pH 7 and ionic strength of 0.06 M. Ionic strength was adjusted with 1 M KNO_3. The measurements were done with three technical replicates.

2.7. Assessment of nanoparticle stability at different pH and high salt concentrations

Stability of nanoparticles at different pH values. Nanoparticles were diluted to 50 µg/ml in buffer solutions with pH ranging from 4 to 10. The following buffers were used: 10 mM acetate buffer, pH 4 and 5; 10 mM sodium phosphate buffer, pH 6, 7, and 8; 10 mM borate buffer, pH 9 and 10. Ionic strength was adjusted to 0.15 M by the addition of NaCl. Nanoparticle size at each pH was measured immediately by DLS. Three replicates were done for each measurement. Nanoparticle suspensions were stored for 7 days in plastic cuvettes, which were placed in a wet chamber. On days 1 and 7 additional size measurements were performed.

Stability of nanoparticles at different salt concentrations. Nanoparticles were diluted to 50 µg/ml in a phosphate buffer, pH 7. The ionic strength of the solution was increased to 0.5, 1, 2, and 3 M by the addition of NaCl. Nanoparticle size was measured by DLS for each salt concentration. Viscosity of NaCl solutions were determined with the aid of viscometer and were 1.265 mPa*s (3 M NaCl), 1.145 mPa*s (2 M NaCl), 0.992 mPa*s (1 M NaCl) 0.983 mPa*s (0.5 M NaCl).

Measurement of nanoparticle zeta potential at different pH. Nanoparticle suspensions were diluted to 50 µg/ml in the following buffers: 10 mM acetate buffer, pH 4 and 5; 10 mM sodium phosphate buffer, pH 6, 7, and 8; 10 mM borate buffer, pH 9 and 10. Ionic strength was adjusted to 0.06 M by the addition of KNO_3. Three technical replicates were performed for each measurement.

2.8. Cell viability study

Venous blood was drawn from three healthy volunteers (from 23 to 31 years old) into heparin-contained vacuum tubes. Peripheral blood mononuclear cells (PBMC) were isolated from blood plasma by density gradient centrifugation with Diacoll (1077 g/L, Dia-M, Russia) at 400 g for 40 min. Isolated cells were washed with Hanks′ Balanced Salt solution three times; then cells were seeded in duplicates into 96-well plates (200 µl per well, 1x106 cells/mL). Thirty microliters of sterilized (see **Section 2.6.**) gelatin nanoparticles diluted in water for injections (WFI) were added into each well. Final concentrations of gelatin nanoparticles were 1000, 250, 62.5, 15.6, and 3.9 µg/mL. The negative and positive controls were WFI and 15% DMSO, respectively (**de Abreu Costa, 2017**). Cells were incubated for 24 h in a humidified atmosphere in the CO_2 incubator (5% of CO_2, +37 °C), stained with propidium iodide (PI) (1 µg/mL, 5 µL for 100 µL of cell suspension) for one minute, and analyzed by flow cytometry. The percentage of PI- (living) cells was determined for each sample.

Monocytes engulfing particles fluoresce in the emission spectrum of propidium iodide (maximum about 615 nm) (**Figure 1**). Therefore, gates for living (PI-) and dead (PI +) cells were set according to unstained samples and positive/negative controls (**Figure 2**).

The granularity of nanoparticles-engulfing cells, and, accordingly, the side light scatter (SSC) parameters increases (**Shin, 2020**). Therefore, the engulfing of particles by monocytes was determined by the geometric mean of side scattering intensity (**Figure S5**).

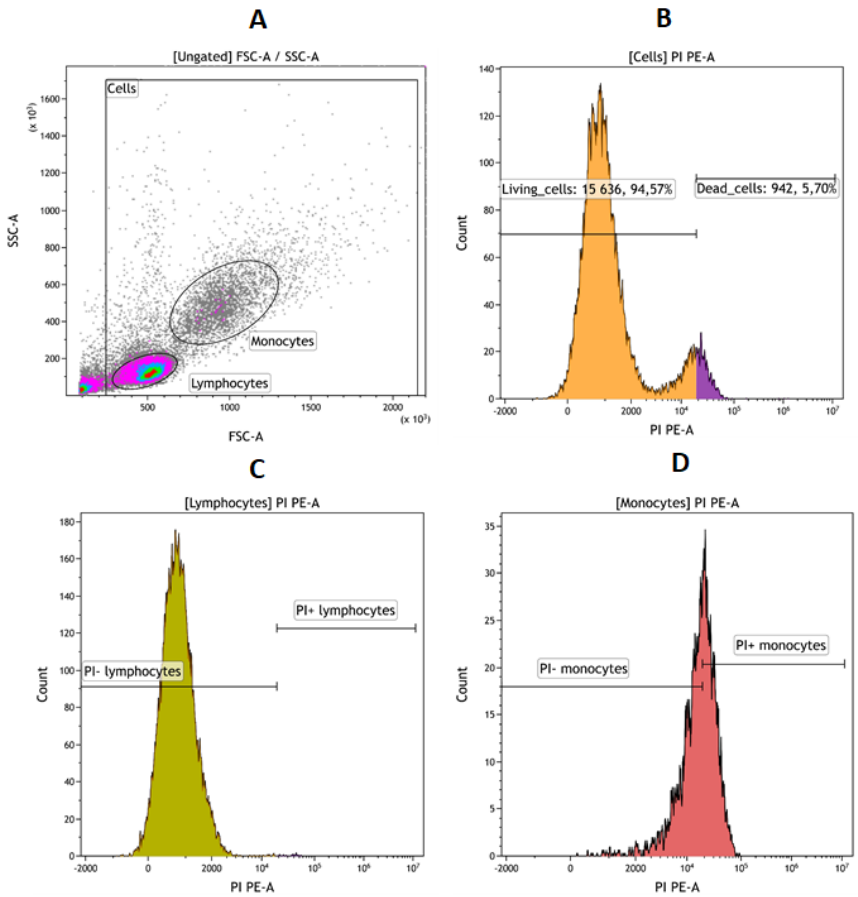

Figure 1. Fluorescence of monocytes engulfing particles in the emission spectrum of propidium iodide in an unstained sample with particles at a concentration of 1000 µg/mL. A - gating of PBMC (cells), lymphocytes, and monocytes on the light scatter dot plot; B - all PBMC are displayed on the histogram; C - the histogram the of lymphocytes gate ; D - the histogram shows the gate of monocytes (some of the cells get into the gate of dead cells, set by unstained control without particles).

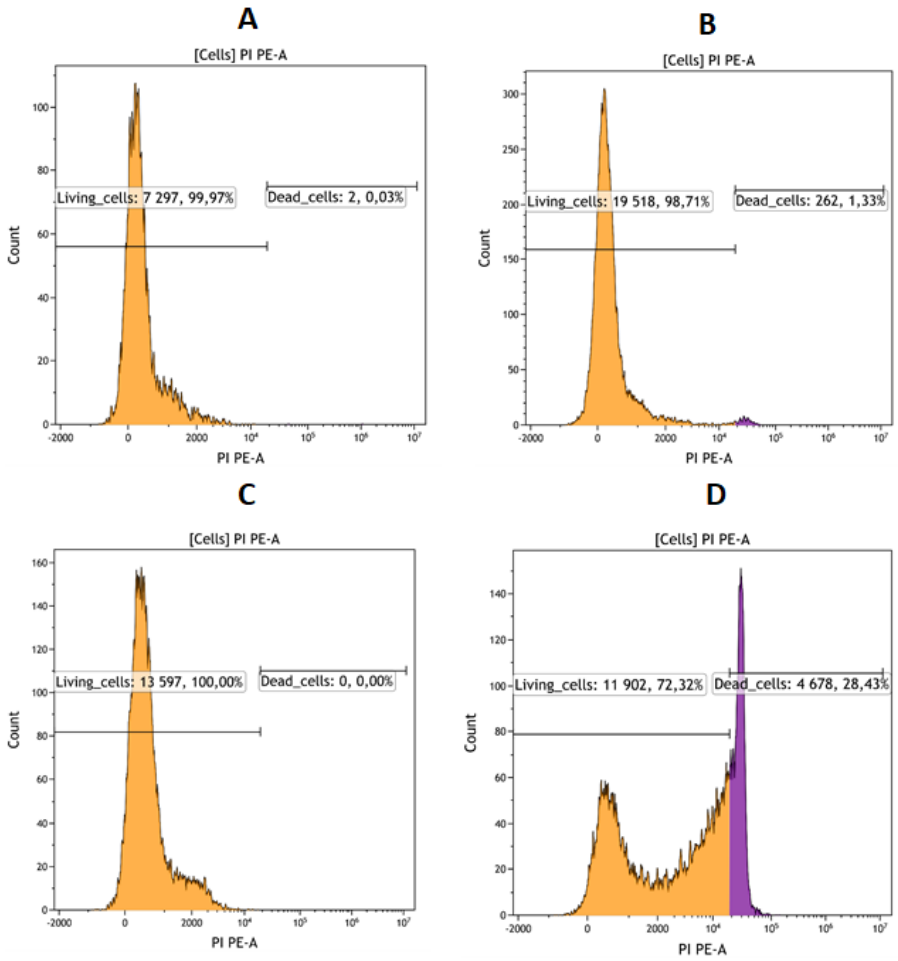

Figure 2. Gating of living and dead cells on unstained and stained controls without particles (A - unstained control with WFI, B - stained control with WFI, C - unstained control with DMSO, D - stained control with DMSO). WFI - water for injections

3. Results and discussion

3.1. Stirring promotes nanoparticle aggregation in the course of desolvation

We revealed that quick one-time addition of non-solvent to aqueous gelatin solution without agitation leads to the formation of monodisperse gelatin nanoparticles. Moreover, in the course of preliminary experiments nanoparticles were successfully prepared from gelatin B with bloom value as low as 75 (molecular weight in the range between 20-25 kDa according to manufacturer). This result contradicts conclusions made by other researchers: usually, removal of low-molecular-weight gelatin fractions is necessary to obtain stable and fine nanoparticle suspensions (**Zwiorek, 2006, Ahlers, 2007**). We suggest that stirring of gelatin solution upon addition of non-solvent promotes aggregation of gelatin molecules and, thus, can be completely omitted.

To prove our suggestion we performed the following experiment. Ethanol was quickly added to gelatin B (75 bloom) solutions (10 and 20 mg/ml). Then, the suspensions were mixed using three regimes: 1) gentle mixing on rotator; 2) slow vortexing; 3) fast vortexing. Three individual batches were prepared for each condition. Their size and polydispersity as well as turbidity (absorbance at 600 nm) were measured immediately after the synthesis.

At the gelatin concentration of 10 mg/ml vortexing has little effect and only the highest speed provokes slight growth of size and turbidity. However, vortexing had a dramatic impact when gelatin concentration was doubled: almost 50% growth of mean size and turbidity at a low speed and severe aggregation at a high speed. At the same time, homogeneous suspensions of gelatin nanoparticles with polydispersity indices lower than 0.1 were formed when mixing was performed on the rotator (**Figure 3**). We did not perform experiments with higher gelatin

concentrations, but recently we successfully prepared gelatin nanoparticles using 30 mg/ml gelatin solution which was desolvated under short gentle mixing (**Khramtsov, 2021**).

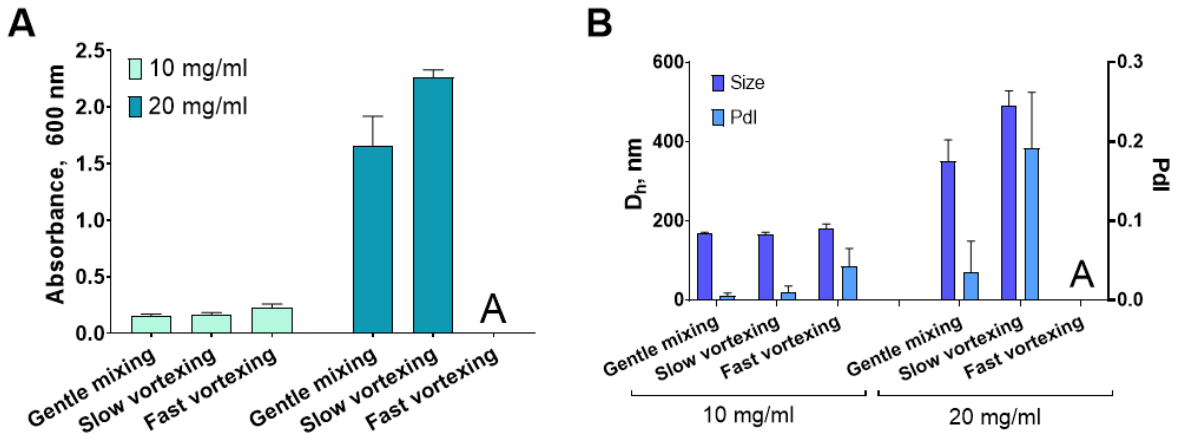

Figure 3. Influence of stirring intensity of the turbidity (A) and size (B) of gelatin nanoparticles. D_h - hydrodynamic diameter, PdI - polydispersity index.

Obtained results explain why some researchers were able to make the one-step synthesis of gelatin nanoparticles without removal of low-weight gelatin fractions (**Farrugia, 1999, Vandervoort, 2004, Kaul, 2002, Kommareddy, 2008, Ofokansi, 2010, Singh, 2016, Esteban-Pérez, 2020**). They desolvated solutions with low gelatin concentrations (1% or less) which are not affected by stirring.

At the same time, Geh et al. synthesized monodisperse gelatin nanoparticles from 40 and 50 mg/ml gelatin solutions by adding acetone under stirring (**Geh, 2016**). The authors used commercially available gelatins A and B with bloom values of 300 and mean molecular weights in the range between 400-500 kDa. Therefore, we suggest that low-molecular-weight fractions in gelatin preparations can promote aggregation in the course of desolvation at high total gelatin concentrations (circa 20 mg/ml and more) when stirring is carried out. A small percentage or absence of low-molecular-weight fractions enables nanoparticle synthesis under stirring. To reinforce previous findings and demonstrate the role of stirring and low-molecular-weight gelatin fractions in the desolvation process two more experiments were performed.

Firstly, we desolvated a solution of low-bloom gelatin B (30 mg/ml, pH 9) with ethanol under vigorous stirring and without stirring. One-time addition of non-solvent lead to homogeneous suspension of nanoparticles whereas stirring-assisted dropwise addition of ethanol resulted in the formation of gelatin bulk at the bottom of the vial (**Figure 4**).

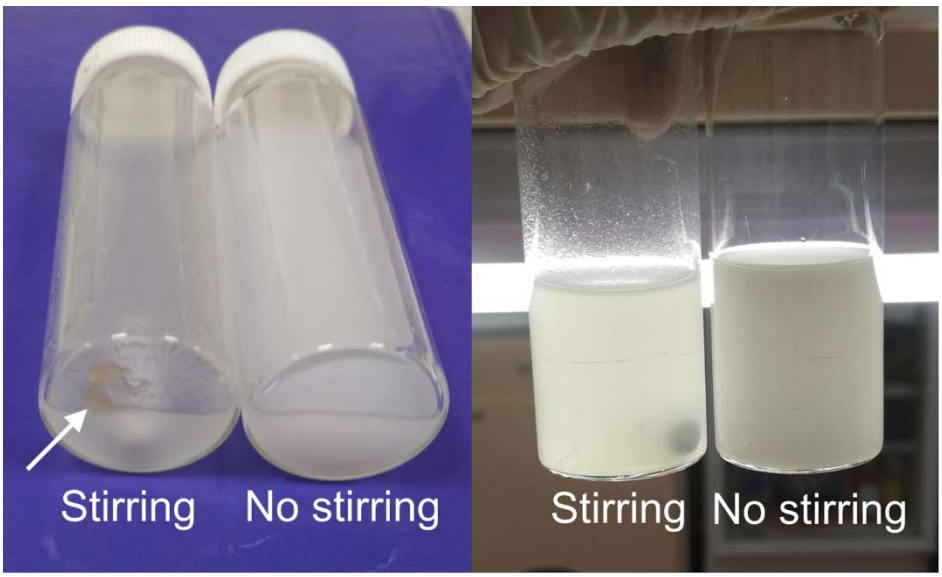

Figure 4. Gelatin nanoparticles prepared from gelatin B, 75 bloom by one-time addition of ethanol without stirring and by dropwise addition of ethanol under stirring. Large gelatin aggregates are labeled with arrows.

In the second experiment, we desolvated with isopropyl alcohol solutions of gelatins A with bloom values of 300 and 62 (both 30 mg/ml, pH 10) or their 3:1, 2:2, or 1:3 mixtures. The total volume of the gelatin solution was 4 ml. Volume fraction of gelatin A, 62 bloom varied from 0% (4 ml of gelatin A, 300 bloom + 0 ml of gelatin A, 62 bloom) to 100% (0 ml of gelatin A, 300 bloom + 4 ml of gelatin A, 62 bloom). As we said before, Geh and colleagues successfully desolvated (**Geh, 2016**) solution of gelatin A, 300 bloom under stirring. Therefore, this sort of gelatin is suitable for one-step desolvation. Conversely, gelatin A, 62 bloom has one of the lowest bloom values from commercially available gelatins and should contain mostly low-molecular fractions, being therefore incompatible with the one-step method. By increasing the percentage of low-bloom bloom gelatin in the mixture of two gelatins we studied the role of low-molecular fractions in the desolvation process.

As expected, stirring-assisted desolvation of gelatin mixtures containing 75% and 100% of gelatin A, 62 bloom resulted in sedimentation of sticky gelatin mass at the bottom of the vials (**Figure 5**). On the contrary, no sign of such aggregation was observed in other vials. Visual inspection revealed that more turbid suspensions were obtained when the percentage of low-bloom gelatin exceeded 25% (**Figure 6**).

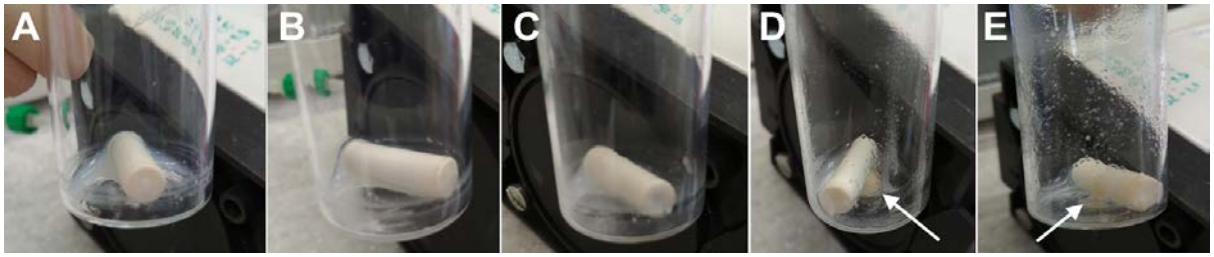

Figure 5. Bottom of the glass vials and magnets after synthesis of gelatin nanoparticles under stirring from the mixtures of gelatins A with bloom values of 300 and 62. A - A300:A62=4:0; B - A300:A62=3:1; C - A300:A62=2:2; D - A300:A62=1:3; E - A300:A62=0:4. Large gelatin aggregates are labeled with arrows.

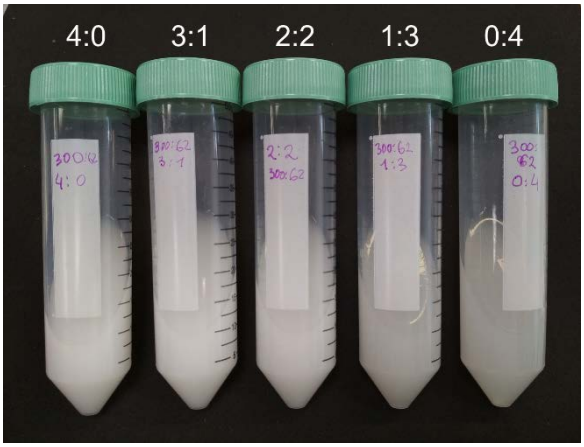

Figure 6. Gelatin nanoparticles prepared under stirring from the mixtures of gelatins A with bloom values of 300 and 62 (see text for details). Corresponding A300:A62 ratios are specified.

After that, we performed desolvation of low-bloom gelatin A solution under stirring and without stirring, as was done previously for gelatin B, 75 bloom. Again, the homogeneous colloidal solution was obtained in the stirring-free conditions, whereas stirring-assisted desolvation resulted in turbid suspension, containing visible aggregates and gelatin mass at the bottom of the reaction vessel (**figure 7**).

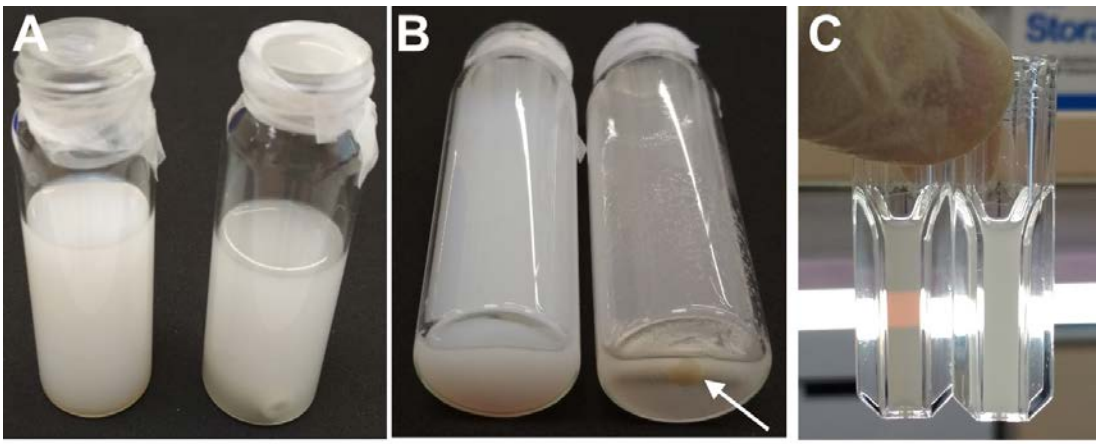

Figure 7. Gelatin nanoparticles prepared from gelatin A, 62 bloom by one-time addition of isopropyl alcohol without stirring and by dropwise addition of isopropyl alcohol under stirring. Large gelatin aggregates are labeled with arrows.

On the basis of the above results, we can conclude that stirring promotes gelatin aggregation in the course of desolvation. Aggregation occurs when low-molecular gelatin fractions are present in sufficient amounts and total gelatin concentration is high (approximately 20 mg/ml and more). These factors make desolvation of medium- and low-bloom gelatins hardly possible to be made in one step when synthesis is carried out in conventional conditions: dropwise addition of poor solvent under stirring. At the same time, the one-time addition of poor solvent with the following short gentle mixing enables the synthesis of gelatin nanoparticles from gelatin with any bloom number.

Dropwise addition of nonsolvent under vigorous stirring is an inevitable part of protein nanoparticle synthesis by the desolvation method. There are many studies reporting a decrease in size and/or polydispersity of albumin (**von Storp, 2012**), silk fibroin (**Matthew, 2020),** α-lactalbumin (**Mehravar, 2011**) nanoparticles at higher stirring speeds. The same findings were provided for gelatin nanoparticles by different research groups (**Subara, 2018, Abdelrady, 2019**). Conversely, Pei et al. (**Pei, 2021**) showed that increase of gelatin concentration in water-ethanol mixture under agitation leads to growth of gelatin nanoparticle size and even to gelation. Removal of low-molecular-weight fractions was not performed in this work as it was aimed at studying gelatin behavior in ethanol-water mixtures rather than the preparation of nanoparticles. Intense shaking provided sedimentation of gelatin 75 bloom in the course of the first desolvation step (**El-Sayed, 2019**). There is no contradiction between these reports. Subara and Abdelrady with colleagues removed low-molecular fractions by traditional first desolvation step and studied the effect of stirring speed performing the second desolvation step whereas Pei and colleagues worked with untreated gelatin. Note that Pei et al. (**Pei, 2021**) used high-bloom gelatins (bloom values of 300 and 320 respectively), which are less susceptible to stirring. We suppose that small amounts of low-molecular fractions in such gelatins can provoke some increase in nanoparticle size, but not aggregation.

Stirring-free desolvation was applied for the preparation of monodisperse silk fibroin nanoparticles by Seib et al. (**Seib, 2013**). The method is to add aqueous silk fibroin solution in acetone in a drop-by-drop manner. However, the same research group reported decreasing the size of silk fibroin nanoparticles when the addition of protein was performed under stirring (**Matthew, 2020**).

We cannot explain why stirring affects gelatin desolvation. Morel et al. studied a mixing-induced aggregation of wheat gluten and proposed that the formation of disulfide and isopeptide bonds as well as hydrophobic interactions can drive aggregation (Morel, 2002). There are few cysteine residues in gelatin molecules (ссылки), therefore most likely other mechanisms are involved.

3.2. Influence of pH, gelatin concentration, type, and volume of desolvating agent on the size and yield of gelatin nanoparticles

In earlier works, factors affecting the synthesis of gelatin nanoparticles were extensively studied (**Zwiorek, 2006, Balthasar, 2005 thesis, Azarmi, 2006, Geh, 2016**). However, the authors of these articles used a conventional technique based on the slow addition of desolvating agents to gelatin solution under stirring. We used a modified desolvation method that relies on the one-time addition of non-solvent to the solution of gelatin. Therefore, we decided to re-evaluate how different factors influence the desolvation outcome. Two sets of experiments were carried out. The first part of the experiments was done using very small volumes of gelatin solution (200 µl) and only one type of gelatin. In the second part, 5 types of gelatin were tested in 20-fold larger volumes.

3.2.1. The first part of optimization experiments

Firstly, we conducted preliminary desolvation experiments only with gelatin B 75 bloom in order to trace the overall relationship between synthesis conditions and nanoparticle characteristics (size, polydispersity, and yield). Due to the large number of samples we minimized the starting volume of the gelatin solution to 200 µl. One of three types of alcohol (methanol, ethanol, or isopropyl alcohol) was added to the gelatin solution, then nanoparticles were cross-linked and washed. We varied pH (from 8 to 10) and concentration (from 8 to 32 mg/ml) of gelatin solution as well as the volume of alcohol (600 and 1000 µl, which gave gelatin to alcohol ratios of 1:3 and 1:5, respectively). Here and in the following experiments, the number of glutaraldehyde molecules was at least in two-fold excess to the number of lysine residues, providing a sufficient degree of cross-linking (**Weber, 2000**). Excess of glutaraldehyde has no significant effect on particle size (**Azarmi, 2006, Ofokansi, 2010**). The addition of diluted glutaraldehyde allowed a decrease in its local concentration and prevented the aggregation of gelatin molecules. Syntheses were made in 2 ml centrifuge tubes, however, the small size of tubes led to imperfect mixing conditions that could affect both the size and yield of nanoparticles. That is why we considered this experiment only as a preliminary study. During the second iteration of experiments, we used larger volumes of reagents (see below in this section) and obtained more consistent results.

The size and yield of nanoparticles decreased with pH increasing when methanol and ethanol were used as non-solvents (**Figures 8 and 9**). Gelatin molecules have a more negative charge at higher pH values which leads to stronger electrostatic repulsion, making them less susceptible to desolvation. Higher volumes of alcohols provided higher yields, which is explained by decreased solubility of protein at a high alcohol concentration (**Yoshikawa, 2012**). Importantly, the desolvating efficiency of isopropyl alcohol is significantly higher (yields varied from 70 to 100%) in comparison with ethanol and methanol. The addition of isopropyl alcohol to 80% (1000 µl) provided quantitative desolvation of gelatin independent of other experimental conditions. Counterintuitive decrease of yield in samples with the lowest gelatin concentration can be explained by loss of nanoparticles during washing steps. Such a loss was inevitable due to low sample volumes and had the highest impact in samples with a gelatin concentration of 8 mg/ml because of the low total amount of gelatin in these samples. In general, smaller nanoparticles were obtained when ethanol and methanol were utilized.

The percentage of gelatin transformed to nanoparticles decreased with the increase of initial gelatin concentrations (except for samples with a maximum volume of isopropyl alcohol), whereas the size of nanoparticles increased. Most of the samples prepared at starting gelatin concentration of 32 mg/ml contained polydisperse microparticles and submicron particles.

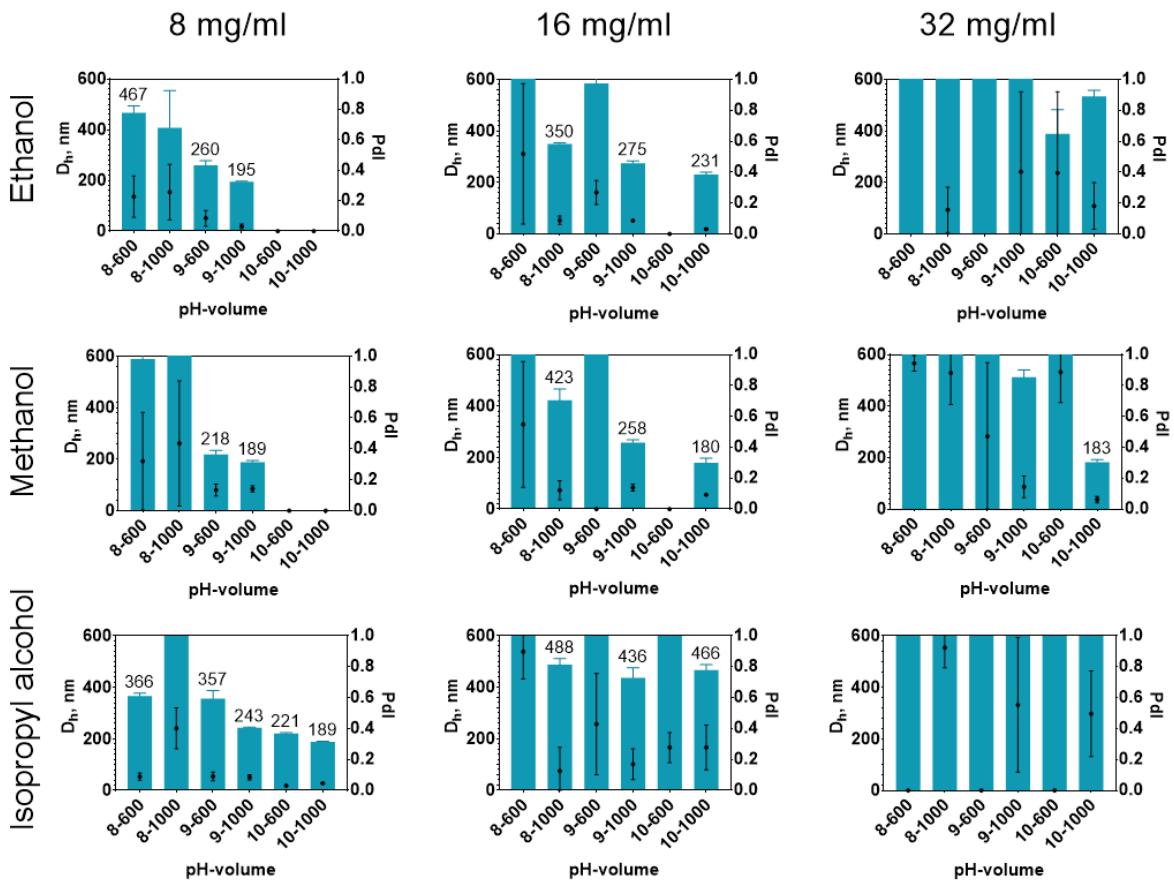

Figure 8. Dependence of the size and polydispersity of gelatin nanoparticles on pH, initial gelatin concentration, and type and volume of desolvating agent. Preliminary experiment, desolvation of 200 µl gelatin B, 75 bloom solution in centrifuge tubes. No bar means that nanoparticles were nor formed. Initial gelatin concentrations are given at the top of the figure. D_h - hydrodynamic diameter, PdI - polydispersity index.

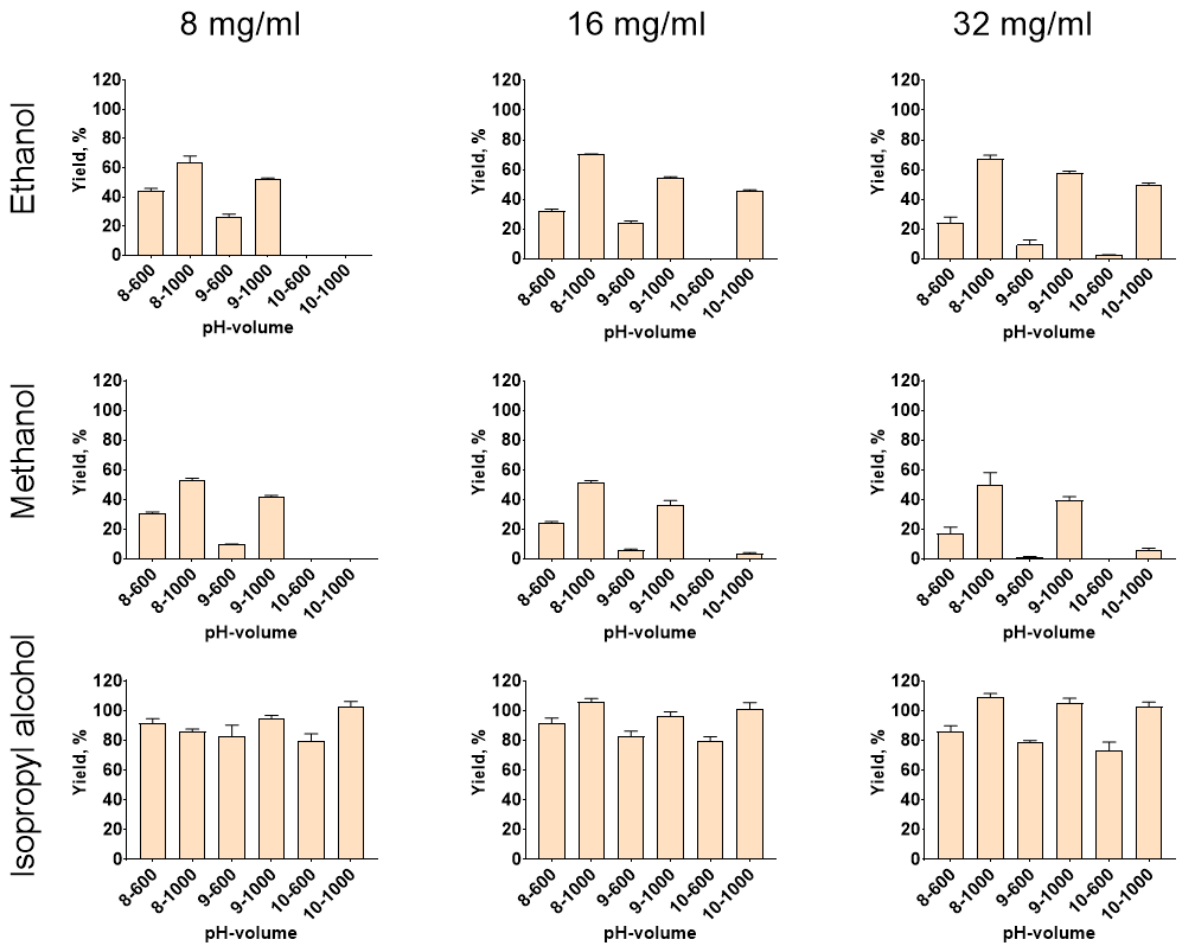

Figure 9. Dependence of the yield of gelatin nanoparticles on pH, initial gelatin concentration, and type and volume of desolvating agent. Preliminary experiment, desolvation of 200 µl gelatin B, 75 bloom solution in centrifuge tubes. No bar means that nanoparticles were nor formed. Initial gelatin concentrations are given at the top of the figure.

3.2.2. The second part of optimization experiments

The addition of methanol and ethanol provided smaller nanoparticles, however, isopropyl alcohol gave higher yields. Therefore in the second part of the experiments, we used ethanol and isopropyl alcohol as desolvating agents. The volume of gelatin solution was increased to 4 ml and synthesis was performed in 50 ml centrifuge tubes to provide better mixing conditions. Higher pH values (9 and 10 for gelatin B; 10 and 11 for gelatin A and fish gelatin) were used to obtain smaller and more homogeneous nanoparticles. Alcohol to gelatin volume ratios were 3:1, 5:1, and 7:1. Gelatin concentrations were 5, 9, and 18 mg/ml. We decided not to use higher gelatin concentrations because aggregation was observed in the preliminary study at a concentration of 32 mg/ml. For some batches of gelatin, nanoparticles yields of more than 100% were obtained. Overestimation probably occurred across all samples and was caused by the interaction of free aldehyde groups located on the nanoparticles' surface with a BCA reagent that was used for gelatin quantification (**Tyllianakis, 1994**). Nevertheless, the general effect of synthesis conditions on the nanoparticle yield still could be assessed.

Surprisingly, much more consistent results were obtained when optimization was conducted at a larger scale. Even at the highest gelatin concentration, monodisperse nanoparticles were obtained, indicating the possibility of further increase of gelatin concentration. Data on the size and yield of nanoparticles are summarized in the **figures 10, 11, S1, and S2.** Only one batch of nanoparticles was prepared for each set of conditions, therefore obtained results are not conclusive. Below we highlight the key findings on the effects of synthesis conditions on nanoparticle properties.

Isopropyl alcohol was a more effective desolvating agent than ethanol. It provided homogeneous nanoparticle suspensions with considerably higher yields. Isopropyl alcohol has

the lowest polarity index and highest dielectric constant in comparison with methanol and ethanol. It has been reported that the desolvation of α-lactalbumin by isopropyl alcohol provided the largest nanoparticles (**Arroyo-Maya, 2012**). moreover, a lower volume of isopropyl alcohol is required to completely desolvate BSA in comparison with ethanol (**Sun, 2018**). A more complex relationship between properties of non-solvent and its influence on the size of nanoparticles, not limited to the difference of dielectric constants, was demonstrated by Mohammad-Beigi et al. (**Mohammad-Beigi, 2016**). Pei et al. assumed that differences in alcohols' viscosity can influence the desolvation of gelatin (**Pei, 2021)**. As a rule, smaller nanoparticles were obtained using ethanol, which is in line with the previous reports (**Sun, 2018**). This difference, though, was more distinct at the gelatin concentration of 18 mg/ml. At lower gelatin concentrations, especially at higher pH, ethanol provided a very low degree of gelatin to nanoparticle transformation, which led to unstable DLS results. Larger volumes of alcohols resulted in higher yields due to the lower solubility of gelatin at higher alcohol. Diameters of nanoparticles became lower, probably because the addition of large alcohol volume decreased the final gelatin concentration. Similar trends were observed by Shamarekh et al. (**Shamarekh, 2020**).

An increase in gelatin concentrations led to the growth of nanoparticle size. This effect was more prominent for gelatins B and fish gelatin at pH 11. The same relationship was reported by different researchers (**Won, 2008, Madkhali, 2018**, **Geh, 2016, Shamarekh, 2020, Pei, 2021**). Probably, a higher local concentration of gelatin favors the desolvation process, which is also illustrated by higher particle yields at the higher protein concentration (**Shamarekh, 2020)**. However, other factors, such as gelatin solution viscosity can also impact desolvation results (**Pei, 2021**).

Higher yields were observed for the same ethanol volume for gelatin B with bloom values of 225 in comparison with gelatin B bloom 75 which is in line with the results obtained by Nixon et al. (**Nixon, 1966**), who showed that lower ethanol volume is necessary to initiate coacervation of gelatins with higher bloom numbers. Interestingly, an opposite relationship was observed for isopropyl alcohol.

Electrostatic repulsion of gelatin molecules and pH-dependent degree of molecule hydration influence both size and yield of nanoparticles as was shown by many researchers (**Ofokansi, 2010, Ahsan, 2017, Ding, 2019, Geh, 2016**). Generally, higher pH values (far away from gelatin isoelectric point) resulted in lower yields and smaller particles.

Obtained results demonstrate that control over synthesis parameters enables tuning of nanoparticles properties and process yield.

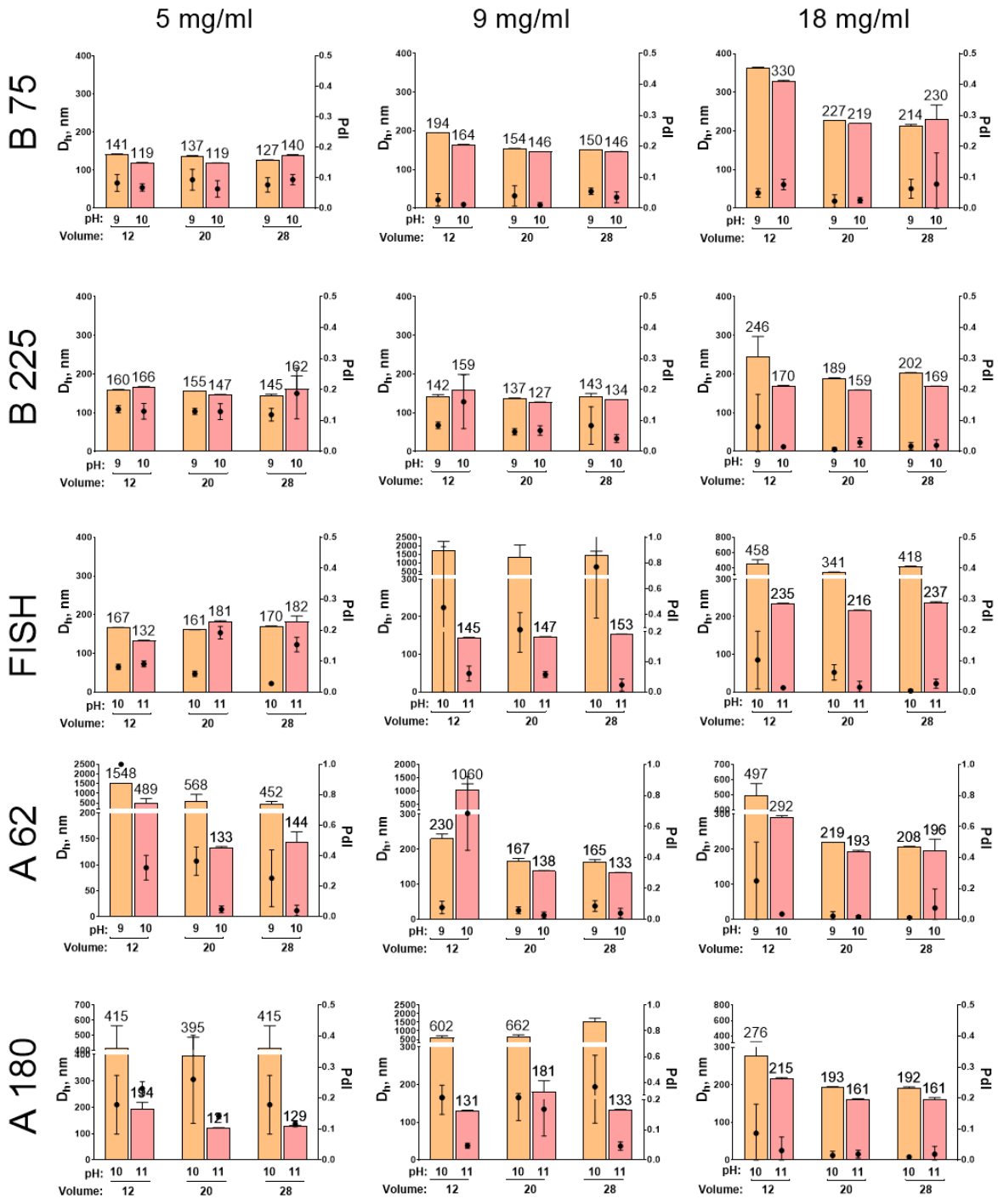

Figure 10. Size of gelatin nanoparticles prepared at different conditions using isopropyl alcohol as a poor solvent. Initial gelatin concentrations are given at the top of the figure. D_h - hydrodynamic diameter, PdI - polydispersity index.

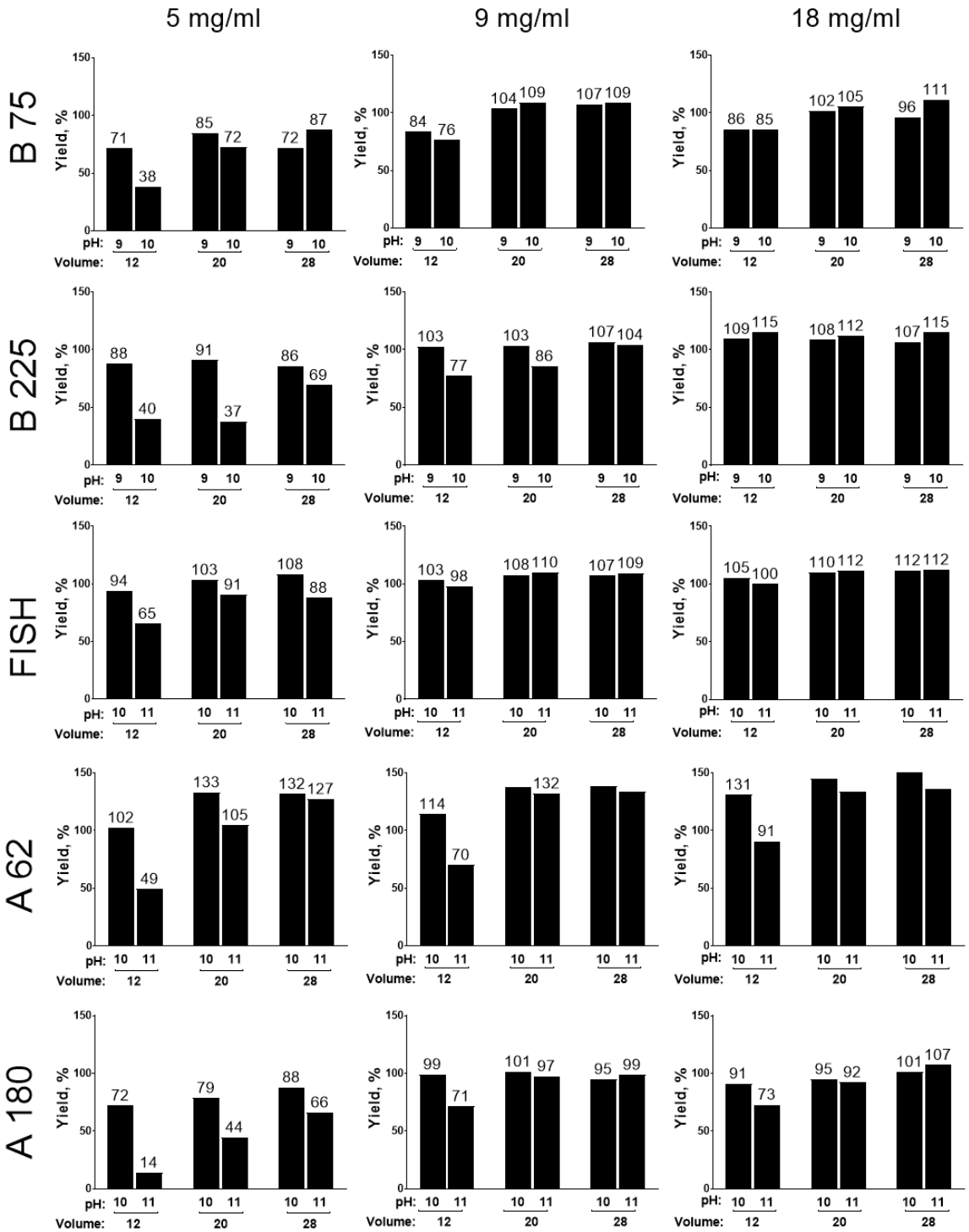

Figure 11. Yield of gelatin nanoparticles prepared at different conditions using isopropyl alcohol as a poor solvent. Initial gelatin concentrations are given at the top of the figure.

3.3. Synthesis of nanoparticles from different gelatins in hundreds of milligram-scale

In order to demonstrate the scope of the modified desolvation method, we synthesized nanoparticles from various types of gelatin with different bloom numbers. On the basis of optimization experiments, we decided to desolvate gelatins with isopropyl alcohol to obtain high yields of nanoparticles. We intended to prepare nanoparticles with hydrodynamic diameters less than 200 nm, hence 10 mg/ml gelatin solutions with high pH were used.

Scalability is an essential part of nanoparticle products implementation. Ideally, the synthesis procedure should be not only scalable but also reproducible, providing small batch-to-batch variability (**Spoljaric, 2021**). Optimization experiments were done using rather small

portions of gelatin (less than 80 mg). Here we performed the hundreds-of-milligram-scale synthesis of gelatin nanoparticles by modified desolation method.

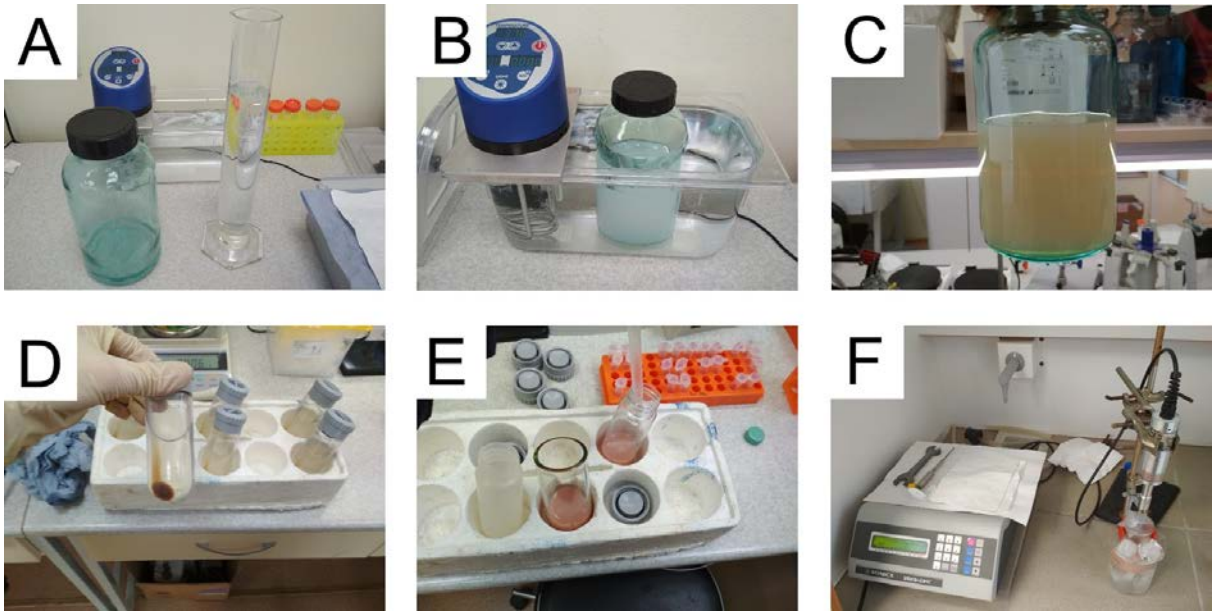

Figure 12. Stages of gelatin nanoparticle synthesis. A - solution of gelatin and isopropyl alcohol before mixing; B - incubation of nanoparticles at the water bath; C - nanoparticle suspension appearance after glutaraldehyde addition; D - sediment of nanoparticles after centrifugation; E - combining of washed gelatin nanoparticles prior to final sonication; F - sonication of gelatin nanoparticles on ice.

We synthesized nanoparticles from porcine, bovine, and fish gelatin with different bloom numbers including the lowest available (62 and 75). The total initial amount of gelatin was 1000 mg, three batches were synthesized for each kind of gelatin. Each batch had an ID, indicating the type of gelatin source and number of replication, e.g. “B225-2”. Key steps of the synthesis procedure are presented in the **figure 12**. Isopropyl alcohol was added to gelatin solution, the resulting suspension of gelatin nanoparticles was kept in the water bath for 30 min, then nanoparticles were stabilized by glutaraldehyde, washed by centrifugation, concentrated, and sonicated. Properties of synthesized nanoparticle batches are summarized in **table 1** and **figure 13**. In total, we confirmed that the modified desolvation method enables nanoparticle synthesis from different gelatin types with various bloom numbers.

Table 1. Properties of gelatin nanoparticles prepared from different gelatins

Batch ID	Suspension volume, ml	Concentration, mg/ml	Total dry weight of nanoparticles, mg[1]	Yield, %	D_h, nm[1]	PdI[2]	Zeta potential, mV
B75-1	45	18,0	810,0	81,0	189±8[3]	0,014±0,007	-11,5±0,6
B75-2	46	17,7	815,6	81,6	171±8	0,030±0,012	-10,2±0,6
B75-3	44	18,2	800,8	80,1	165±4	0,033±0,029	-10,7±0,6
B225-1	45	13,8	621,0	62,1	133±4	0,069±0,022	-11,5±0,5
B225-2	45	14,4	646,2	64,6	139±6	0,094±0,034	-10,9±0,3
B225-3	45	15,2	685,4	68,5	143±5	0,127±0,065	-11,1±0,6
FISH-1	46	17,8	817,0	81,7	164±7	0,114±0,047	-9,0±1,0
FISH-2	46	16,9	778,8	77,9	156±6	0,094±0,052	-9,4±0,3

FISH-3	46	16,9	775,6	77,6	151±3	0,107±0,029	-7,1±0,8
A62-1	46	16,9	777,4	77,7	157±8	0,054±0,012	-7,9±0,9
A62-2	45	16,4	738,0	73,8	148±4	0,064±0,012	-7,8±1,3
A62-3	45	14,5	652,5	65,3	151±4	0,052±0,004	-7,5±0,4
A180-1	45	15,8	711,0	71,1	144±3	0,088±0,023	-7,1±0,7
A180-2	46	17,0	782,0	78,2	142±2	0,060±0,014	-6,9±0,7
A180-3	45	17,1	769,5	77,0	145±4	0,087±0,036	-7,4±0,6

[1] - Hydrodynamic diameter
[2] - Polydispersity index
[3] - Mean of 3 technical replicates ± standard deviation

3.3.1. Size, zeta potential, and shape of nanoparticles

The hydrodynamic diameter of most nanoparticles was between 130 and 160 nm. The lowest nanoparticles were prepared from gelatin B, 225 bloom. We assessed the reproducibility of nanoparticle synthesis by calculating coefficients of variation (CV) for each type of gelatin and comparing it with available literature data. Reproducibility was the lowest for nanoparticles prepared from gelatin B, 75 bloom (CV=7.2%), whereas for other gelatin types CVs were from 1.2% to 4.4%. Reproducibility of the preparation of recombinant human serum albumin nanoparticles by desolvation method was studied by Langer et al. Three batches were prepared, CV was 9.1% (**Langer, 2008**). Gelatin nanoparticles of different sizes prepared by optimized two-step desolvation were reported by Dr. Claus Zwiorek (**Zwiorek, 2006**). Six batches were synthesized for each type of gelatin nanoparticles, coefficients of variation were 3.4% (mean size is 300 nm), 1.4% (150 nm), 13.2% (100 nm). Thus, the modified desolvation method enables the reproducible synthesis of gelatin nanoparticles. Polydispersity indices were lower than 0.2 for all batches and lower than 0.1 for most batches, indicating that synthesized nanoparticles had homogeneous size distribution.

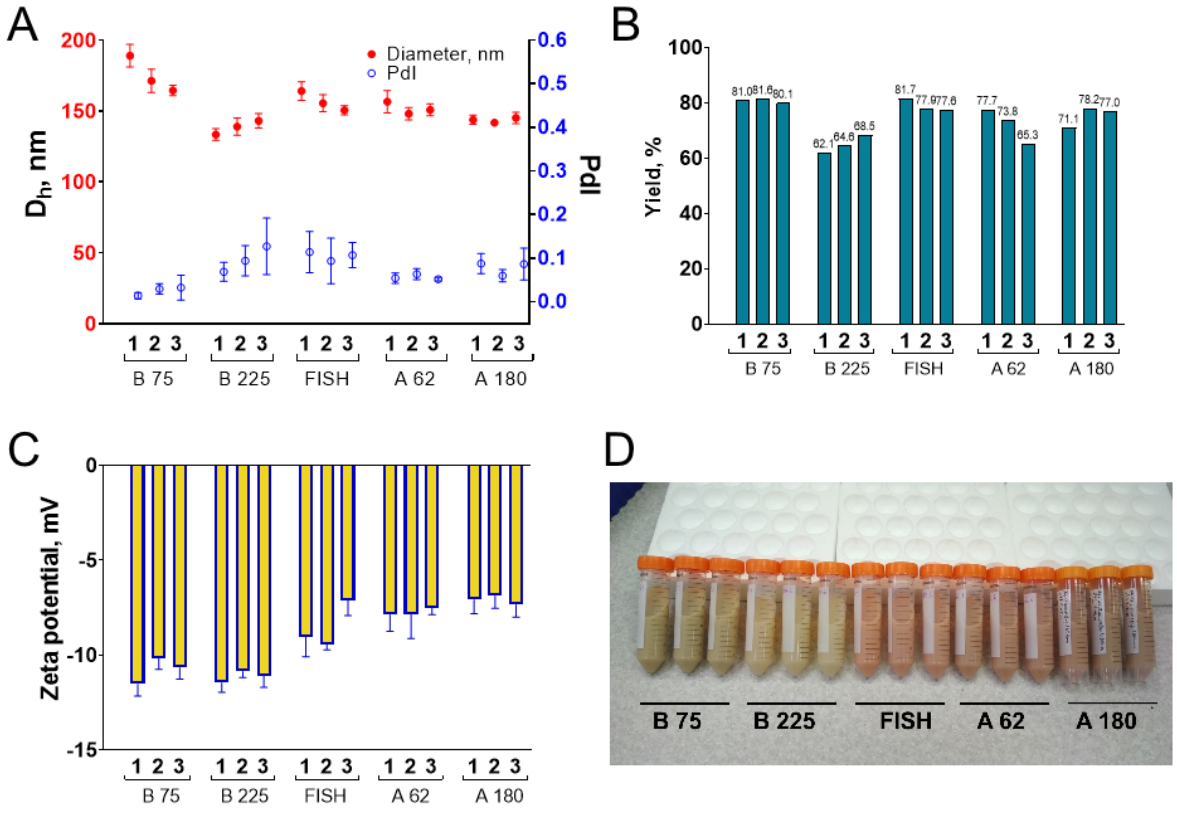

Figure 13. Properties of gelatin nanoparticles prepared from various gelatins in the hundreds-of-milligram scale: A - size and polydispersity index; B - yield; C - zeta potential (at a pH 7); D - the appearance of gelatin nanoparticle suspensions. Numbers 1, 2, and 3 denote the batch numbers. D_h - hydrodynamic diameter, PdI - polydispersity index.

The zeta potential of nanoparticles was measured in a neutral phosphate buffer, pH 7. According to information from the manufacturer, the isoelectric point is 4.7-5.3 for gelatins B, 7.0-9.5 for gelatins A, and 6.0 for fish gelatin. Nanoparticles prepared from gelatin B had the lowest zeta potential of about -11 mV, whereas nanoparticles made from fish gelatin and gelatin A had more positive zeta potential: from -7 to -9 mV. Notably, the zeta potential of gelatin nanoparticles is much lower than the conditional stability threshold of ±30 mV (**Lowry, 2016**), indicating that forces other than electrostatic repulsion provide their colloidal stability, which is confirmed by the results of their detailed colloidal stability study (see **section 3.4.**).

Scanning electron microscopy showed that nanoparticles prepared from all types of gelatin had a round shape (Figure 14). The insufficient quality of SEM photographs did not allow us to measure their sizes. Nevertheless, a visual assessment of the photos demonstrated that the sizes of most of the particles are in the range of 100-200 nm, which coincides with the DLS results. Microscopy demonstrated the presence of large nanoparticles (they can be seen in **Figure 14B**) and some amount of aggregates, however in general nanoparticles are homogeneous.

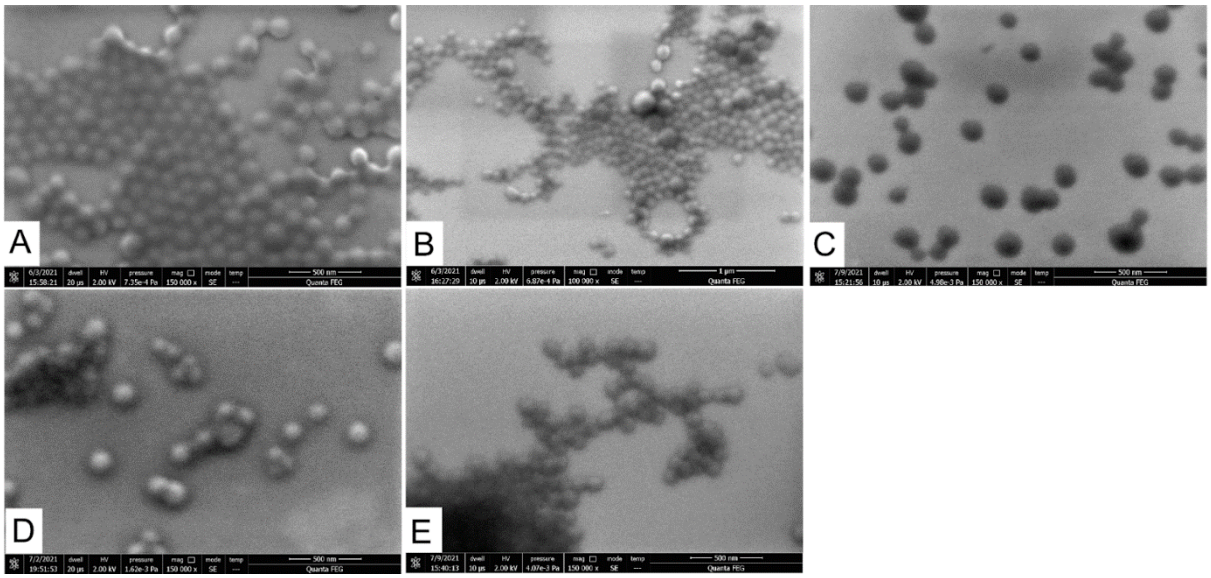

Figure 14. SEM images of gelatin nanoparticles. A - B75-1; B - B225-1; C - FISH-1; D - A62-1; E - A180-1. Scale bars are 500 nm (A, C-E) or 1000 nm (B).

3.3.2. Yield

We obtained stable aqueous suspensions of gelatin nanoparticles having volumes of 44-46 ml and containing from 13.8 to 18.2 milligrams of nanoparticles per milliliter. Therefore, the method allows the preparation of 600-800 mg of nanoparticles in 6-7 hours. This value can be increased by the application of larger reagent volumes or by changing the synthesis conditions: decreasing the pH, increasing the gelatin concentration, and so on (see the section “Influence of pH”). The yield of synthesis (degree of gelatin-to-nanoparticles conversion) was between 62 and 82%, which is higher than reported for two-step and one-step desolvation: 1.5%-62% (**table S1**). However, in special conditions yields of conventional one- and two-step desolvation procedures can reach 70-80% (**Balthasar, 2005 thesis, Balthasar, 2005 biomater, Geh, 2016**). For the nanoprecipitation method yields as high as 90±5% were reported (**Leo, 1997),** however lower yields were obtained in other works (**table S1**). Based on optimization experiments, we claim that

yields up to 95% can be reached with the aid of the modified desolvation method due to the high desolvating efficiency of isopropyl alcohol. In the desolvation technique, there is sometimes a trade-off between the yield and size of nanoparticles. Conditions that favor protein desolvation provide better yields, but the larger size of nanoparticles. An increase in yield can be achieved by lowering the pH or by an increase of added alcohol volume. The second approach enables higher yields and even lower sizes, but at the expense of reaction volume increase. In this work we synthesized gelatin nanoparticles at high pH (10 for gelatin B and 11 for fish gelatin and gelatin A), besides non-solvent to gelatin volume ratio was 5. Using lower pH and/or larger ratios, higher yields could be achieved.

One more thing which needs to be explained is lower yields obtained for B225 batches. We think that losses of nanoparticles during washing steps can be the reason. Nanoparticles B225-1/2/3 had the lowest diameters and required more time to complete sedimentation. When decantation of the supernatant was performed, the loose part of the sediment was removed. This was observed for all batches but in the case of B225-1/2/3 it was the most pronounced.

3.3.3. Absorbance and fluorescence spectra of gelatin nanoparticles

Protein nanoparticles cross-linked with glutaraldehyde emit fluorescence when excited by UV or visible light (**Cai, 2016, Khramtsov, 2021**). Autofluorescence of gelatin nanoparticles can be explained by the presence of C=C (resulting from glutaraldehyde polymerization) and C=N bonds (in the Shiff bases) in nanoparticles' structure (**Wei, 2007**). Fluorescent properties of gelatin nanoparticles can be utilized in bioimaging and biosensing (**Cai, 2016)**. Moreover, intrinsic fluorescence of nanomaterials could be used to measure their cellular uptake (**Tsai, 2011, Singh, 2011**) and underlines nanoparticle interference with various fluorescent techniques (an example of such interference can be found in the **Section 3.8.**). Given that gelatin nanoparticles do not have distinct absorbance peaks (**Figure 15A**), we recorded the fluorescence spectra of nanoparticles at excitation wavelengths from 260 to 560 nm. Color of gelatin nanoparticles depended on synthesis conditions. Desolvation by ethanol at any pH values or by isopropyl alcohol at pH less than 11 resulted in yellowish suspension. Nanoparticles prepared at pH 11 using isopropyl alcohol were reddish, indicating possible differences in the chemical structure.

Nanoparticles prepared from all gelatins possess broad fluorescent peaks, which are red-shifted with the increase of excitation wavelength (**Figure 15B and Figure S3**). Further, we used fluorescent properties of gelatin nanoparticles to assess the change of their structure after the sterilization procedure (see **Section 3.7.**).

.

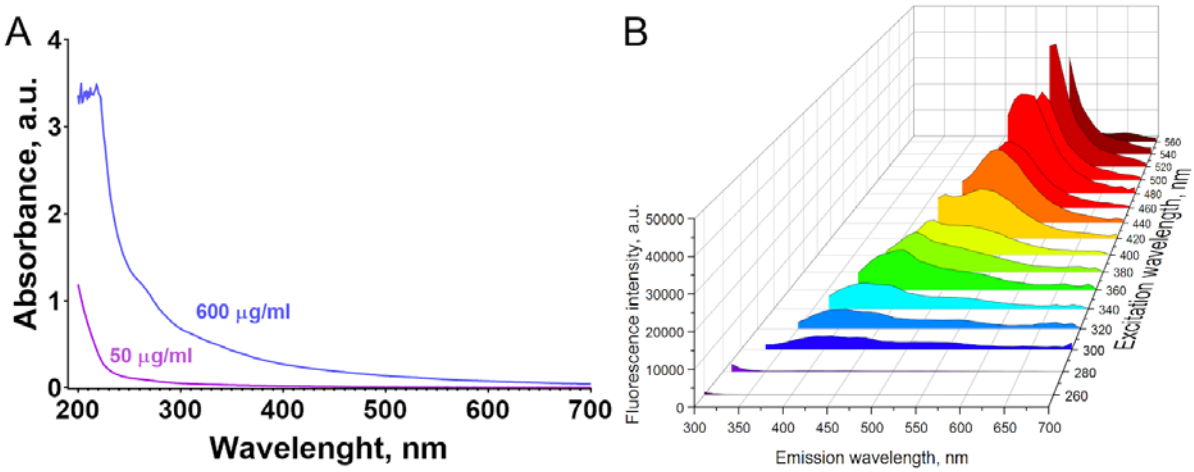

Figure 15. A - absorbance spectrum of B75-1 nanoparticles in water. The final concentration of nanoparticles is 50 and 600 μg/ml. B - emission spectra of B75-1 nanoparticles at various excitation wavelengths.

3.4. pH and salt stability

Colloidal stability of nanoparticles at various pH and in solutions with high ionic strength is highly desirable for practical applications. Conjugation of nanoparticles with different molecules, including recognition molecules (e.g. monoclonal antibodies) as well as a surface modification

with stealth or protecting polymers, are usually performed at pH and salt concentration, which are optimal for a specific technique. Therefore we tested colloidal stability of nanoparticles in buffers with pH ranging from 4 to 10 measuring their size by DLS immediately after addition to the buffer, then at days 1 and 7. Gelatin nanoparticles prepared from gelatin B, fish gelatin, and gelatin A 180 bloom were stable for one week in all buffers (**Figure 16**). A slight increase of size and polydispersity was, though, observed in several samples. In these samples usually, one of three technical replicates indicated the presence of aggregates, whereas other replicates showed homogeneous size distribution. Most likely, insignificant aggregation took place, however, most of the particles were in the non-aggregated state. These results coincide with literature data, indicating that the gelatin shell provides good colloidal stability in the wide range of pH values (**Sivera, 2014**).

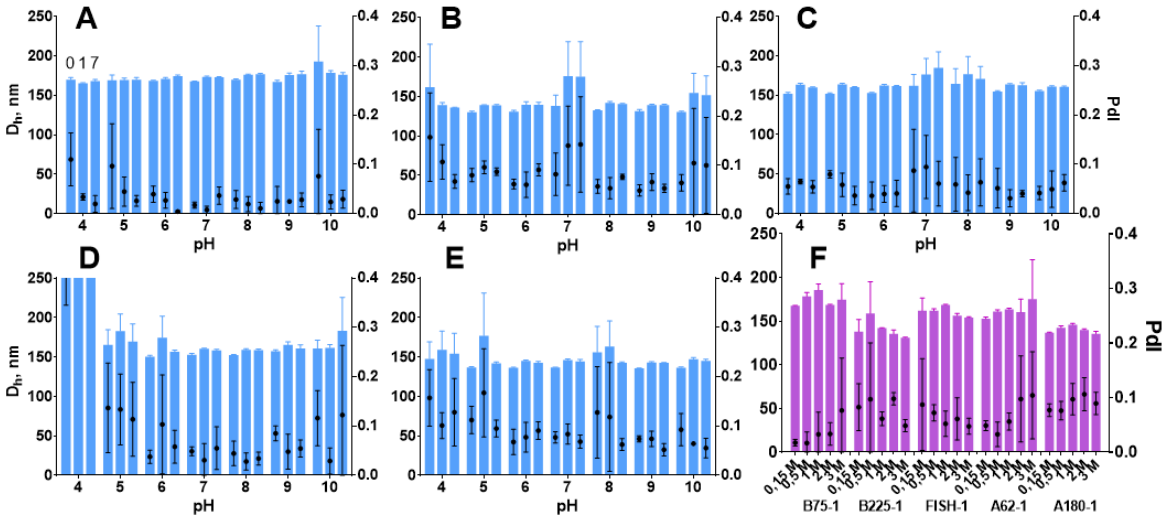

Figure 16. Colloidal stability of gelatin nanoparticles at different pH values (A-E) and salt concentrations (F). A - B75-1; B - B225-1; C - FISH-1; D - A62-1; E - A180-1. D_h - hydrodynamic diameter, PdI - polydispersity index.

Nanoparticles prepared from gelatin A with a bloom value of 62 were the only type of nanoparticles for which pronounced aggregation was observed (**Figure 16D**). These nanoparticles quickly aggregated being exposed to pH 4, but not in other buffers. The relationship between zeta potential and pH was different for nanoparticles prepared from various types of gelatin (**Figure 17**). Nanoparticles B75 and B225 had more negative zeta potential at a pH range from 5 to 9 which is explained by the difference in isoelectric points between gelatins (**Azarmi, 2006**).

High salt concentrations had no significant effect on the size of gelatin nanoparticles. It was previously shown that low (7-50 mM), but not high (300 mM) NaCl concentrations promote aggregation of gelatin nanoparticles (**Fuchs, 2010**). We did not observe any signs of nanoparticle aggregation in presence of salts.

We should note that the concentration of nanoparticles was as low as 50 ug/ml. Perhaps, more pronounced aggregation could be detected at higher particle concentrations. For nanoparticles A180-1/2/3 we detected aggregation at a low nanoparticle concentration (lower than 80 µg/ml) in water, but not in phosphate buffer. Glycine treatment stabilized these nanoparticles even at low concentrations. We cannot explain this phenomenon, moreover, it was not observed for nanoparticles prepared from other types of gelatin.

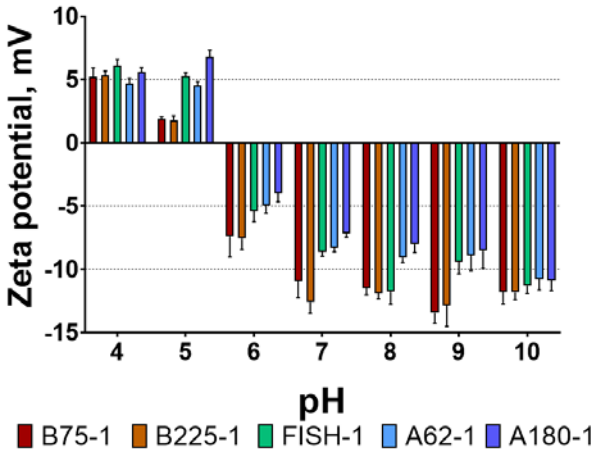

Figure 17. Zeta potential of gelatin nanoparticles at the different pH values.

3.5. Storage stability

The stability of nanoparticles upon storage is necessary for their practical application in any field. For end users concentrated aqueous suspension is, perhaps, the most convenient form of nanoparticle preparations. We studied the size and structural integrity of gelatin nanoparticles prepared using a modified desolvation method after 4 weeks of storage in water at +4 °C. Surprisingly, a decrease in hydrodynamic diameter and polydispersity indices were detected for all batches (**Figure 18**). Moreover, after 4 weeks of storage batch-to-batch variability of nanoparticle sizes also became lower. These unexpected results contradict the data reported in the literature. Previous works reported no change or growth of nanoparticle diameter (**Coester, 2000, Shilpi, 2017**). The decrease of hydrodynamic diameter of gelatin nanoparticles stored in the lyophilized state was observed and explained by incomplete rehydration (**Geh, 2018 thes**), however, in our study nanoparticles were stored in water and did not change hydration state. We supposed that partial dissolution of nanoparticles could occur. The concentration of free protein in nanoparticle suspension, as well as turbidity of nanoparticle suspension, were monitored (**Figure 19**). Turbidity can reflect both the change of nanoparticle size and their dissolution. For almost all nanoparticles, a decrease in suspension turbidity was observed . The concentration of free gelatin was also higher on the 28th day. However, the relative amount of free protein did not exceed 1% of total gelatin.

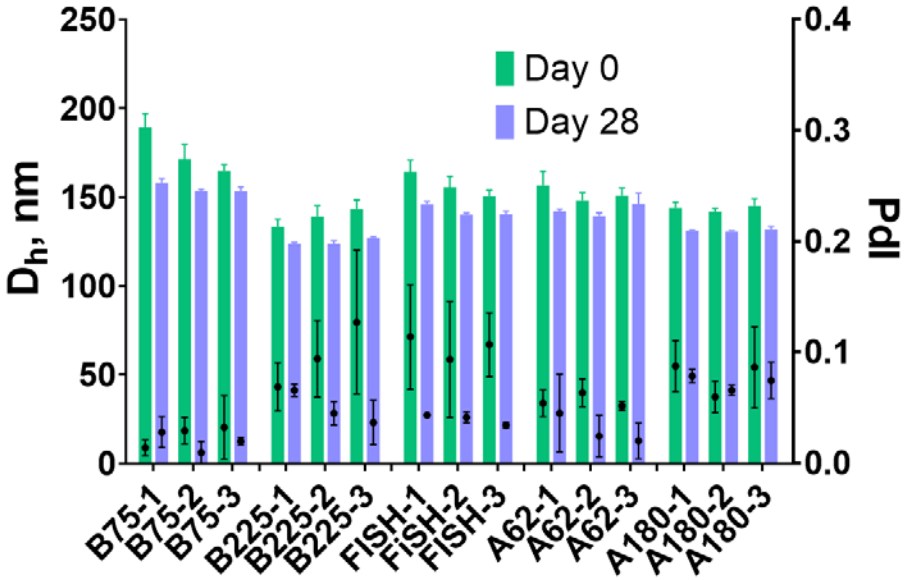

Figure 18. Size (D_h) and polydispersity index (PdI) of gelatin nanoparticles after the synthesis and in 28 days

It can be assumed that the storage of gelatin nanoparticles is accompanied by partial disintegration. Between-batch size variability after 4 weeks of storage became lower, indicating that this process affects larger nanoparticles and aggregates. The percentage of free gelatin was quantified by centrifugation of nanoparticles at 20000 g and measurement of protein in supernatant. Mentioned speed is not high enough to pellet small nanoparticles (say, 10-20 nm). Therefore the slight increase of protein concentration in supernatants can be explained by both the release of single gelatin molecules and the decomposition of larger nanoparticles into smaller ones. The presence of a certain amount of smaller nanoparticles (in contrast to larger nanoparticles) cannot affect the results of DLS measurements, because their light scattering ability is too small. Taking into account that the degree of turbidity decrease did not correlate with the degree of the particle diameter decrease, we assume that partial decomposition of nanoparticles into smaller nanoparticles took place.

Literature data suggest that glutaraldehyde cross-linking produces stable gelatin nanoparticles (**Coester, 2000, Shilpi, 2017**), however, in most cases, only particle size but not other properties were assessed. We examined the storage stability of non-sterile nanoparticle preparations, which were stored in deionized water without any preliminary physical or chemical treatment. Therefore, bacterial contamination and protease activity play a role in nanoparticle degradation. Undoubtedly, further study of nanoparticle stability needs to be conducted. However, even if nanoparticles are unstable in suspension, there are optimized methods of their storage in freeze-dried conditions (**Geh, 2018 thes**).

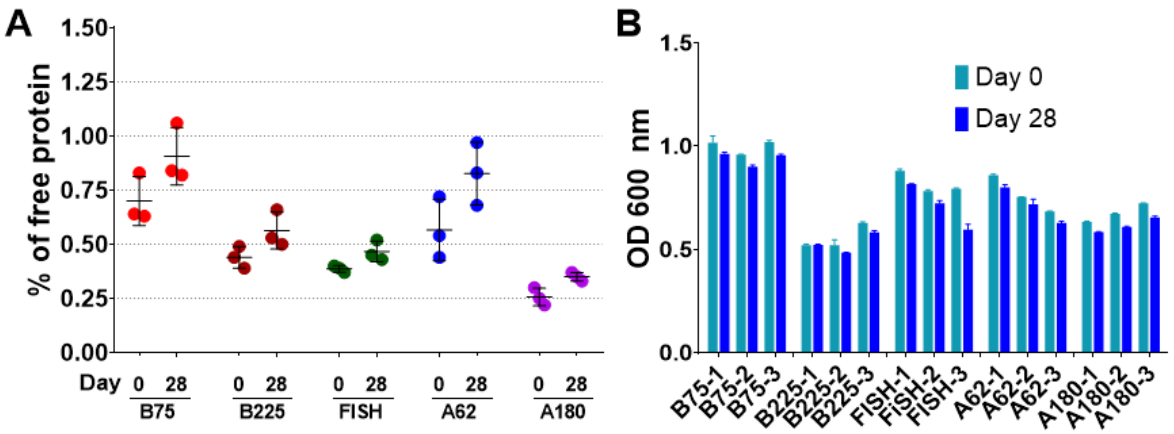

Figure 19. Storage stability of gelatin nanoparticles: A - the percentage of free protein in relation to nanoparticle concentration; B - turbidity of gelatin nanoparticle suspensions at days 0 and 28.

3.6. Loading of gelatin nanoparticles with fluorescent complex

Biomedical and biotechnological applications of gelatin nanoparticles require them to be loaded with a wide spectrum of therapeutic and imaging agents: small molecules, nanomaterials, and polymers. We tested whether the modified desolvation method is appropriate for incorporation of model hydrophobic substance: fluorescent complex containing europium ion and two chelating ligands, namely 1,10-phenanthroline and 4-(4-Methylphenyl)-2,4-dioxobutanoic acid. Europium and ligands were dissolved in ethanol; then gelatins of each type were desolvated with the resulting solution. Ethanol was chosen because of the insufficient solubility of fluorescent complexes in isopropyl alcohol. Europium complexes possess bright fluorescence facilitating confirmation of successful loading, besides they are insoluble in water resembling small molecules used in drug delivery. Moreover, the long-living and large-Stokes-shift fluorescence of europium complexes is easily distinguishable from the inherent fluorescence of gelatin nanoparticles.

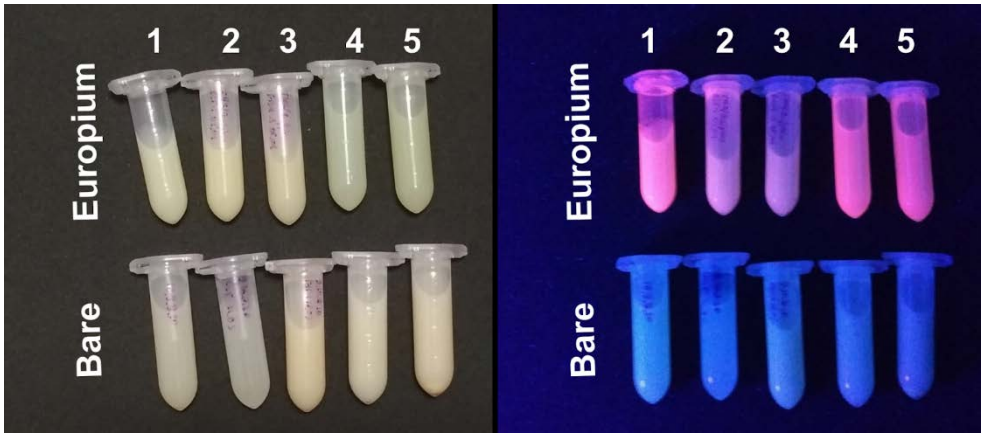

Figure 20. Gelatin nanoparticles containing and not containing europium complexes at daylight (left) and in UV light (360 nm, right). Nanoparticles were prepared from gelatin: 1 - B, 75 bloom; 2 - B, 225 bloom; 3 - FISH; 4 - A, 62 bloom; 5 - A, 180 bloom.

Nanoparticles synthesized from all the gelatin types were loaded with fluorescent complexes (**Figure 20**). A narrow peak (600-630 nm) of europium emission was detected in suspensions of purified gelatin nanoparticles after desolvation with an ethanol solution containing fluorescent complexes (**Figure 21**) but was not detected in bare gelatin nanoparticles (**Figure 20**). Supernatants obtained during the purification of fluorescent gelatin nanoparticles displayed weak fluorescence, which, nevertheless, was negligible in comparison with that of nanoparticles. Therefore, europium complexes were associated with gelatin nanoparticles, however, we did not study whether they were located on the surface or were embedded in the nanoparticle body. Weak fluorescence in supernatants was most likely due to the leakage of fluorescent complexes induced by ultrasound treatment which accompanied nanoparticle purification.

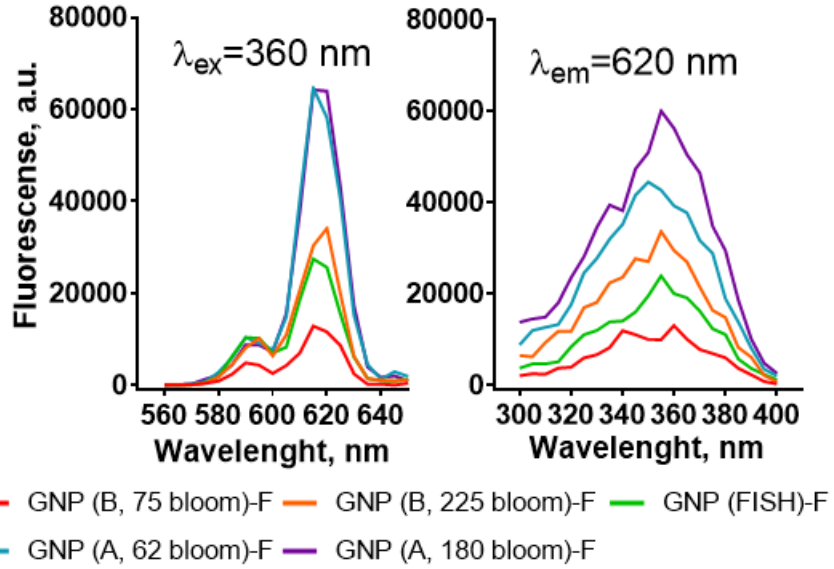

Figure 21. Emission and excitation spectra of gelatin nanoparticles loaded with europium complexes. Nanoparticles prepared from gelatin B, 75 bloom were diluted 1:1000, other nanoparticles were diluted 1:100.

We should note that sub-micro particles and microparticles rather than nanoparticles were synthesized from fish gelatin and type A gelatins (**Figure 22**). Type B gelatin 75 bloom yielded the highest quality nanoparticles with the lowest polydispersity indices. These nanoparticles also had the brightest luminescence.

In this work we did not optimize loading conditions, only a couple of preliminary experiments were carried out with type B gelatins. We suppose that proper optimization can enable the preparation of 100-200-nm-sized nanoparticles loaded with hydrophobic molecules from any type of gelatin.

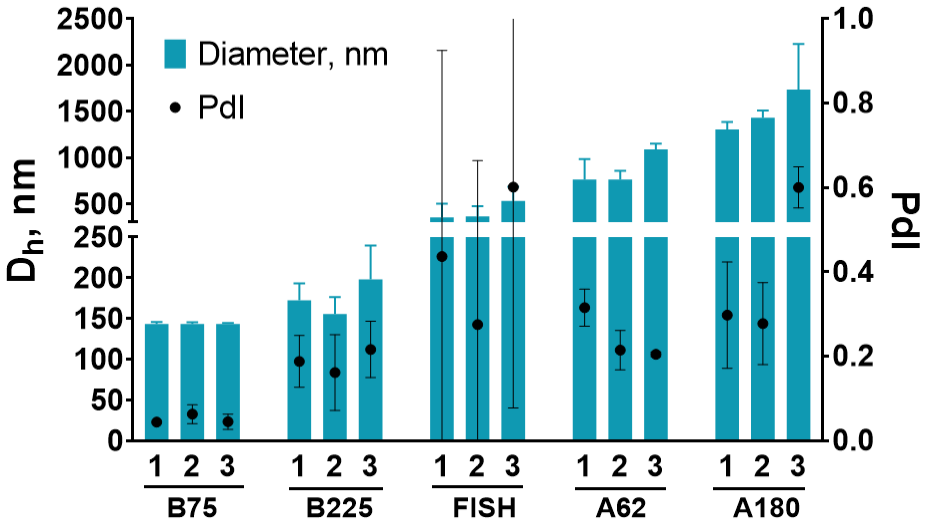

Figure 22. Size of gelatin nanoparticles loaded with fluorescent europium complexes. D_h - hydrodynamic diameter, PdI - polydispersity index.

3.7. Sterilization of gelatin nanoparticles

Microbial contamination of gelatin nanoparticles is undesirable for almost all applications. The presence of microorganisms or their fragments in the nanoparticle preparations could pose a risk for patients, besides microbial enzymes can destroy nanoparticles and decrease their shelf-life (**Vetten, 2014**). Geh et al. reported that autoclave sterilization of gelatin nanoparticles leads to the partial release of gelatin molecules and slight nanoparticle growth, whereas the higher cross-linking degrees and milder autoclaving conditions make nanoparticles less sensitive to thermal degradation (**Geh, 2018 thesis**). At the same time, Ma et al. successfully autoclaved bovine serum albumin nanoparticles prepared by the desolvation method (**Ma, 2016**). Based on these results we decided to sterilize gelatin nanoparticles by autoclaving in the mildest conditions: 15 min at 0.5 atm above atmospheric pressure. Control (non-autoclaved) nanoparticles were kept at +4 °C.

In autoclaving experiments, we used gelatin nanoparticles treated with glycine. Despite we added an excess of glutaraldehyde in relation to the number of primary amines, a small portion of unreacted amino groups can remain on the outer surface of nanoparticles (**Langer, 2000**). Glycine quenched free surface carbonyl groups and supposedly decreased the probability of their reaction with remaining primary amines. Unfortunately, glycine treatment led to unstable DLS measurements. DLS results were different even between technical replicates: for some samples, one or two of three measurements indicated the presence of aggregates or increase of average diameter, whereas other measurements showed narrow distribution. This feature of the DLS method was previously well illustrated by Langevin and co-authors (**Langevin, 2018**). They put TiO2 nanoparticles in a buffer with high ionic strength and measured the diameter of nanoparticles by DLS and differential centrifugal sedimentation, which is much less sensitive to the presence of aggregates than DLS. A large number of aggregates was detected by DLS, on the contrary PCS showed that the agglomeration degree was not significant.

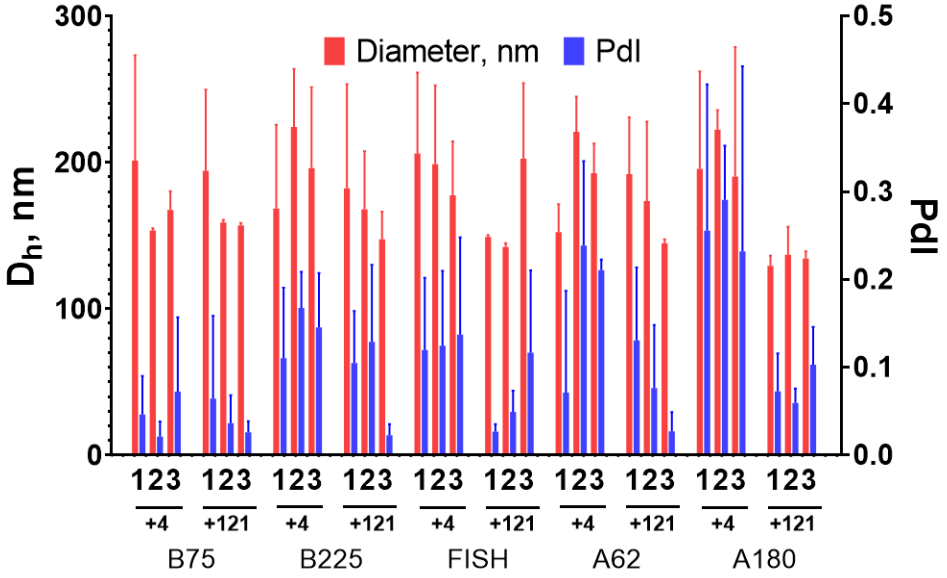

Figure 23. Size (D_h) and polydispersity index (PdI) of non-autoclaved (+4) and autoclaved (+121) gelatin nanoparticles.

To obtain more stable DLS results we centrifuged autoclaved nanoparticles for 10 min at 1000 g before the size measurements (**Figure 23**). We suppose that slight aggregation occurred however most of the particles withstood sterilization and kept their original size because no visible signs of aggregation were detected (**Figure 26**). The presence of aggregates and free gelatin may be incompatible with applications, which require very homogeneous nanoparticle preparations (e.g. drug delivery). However, autoclaving may be a good and simple choice in the fields with less strict requirements to size distribution. Aggregates can be quickly removed by low-speed centrifugation using commonly available sterile centrifuge tubes.

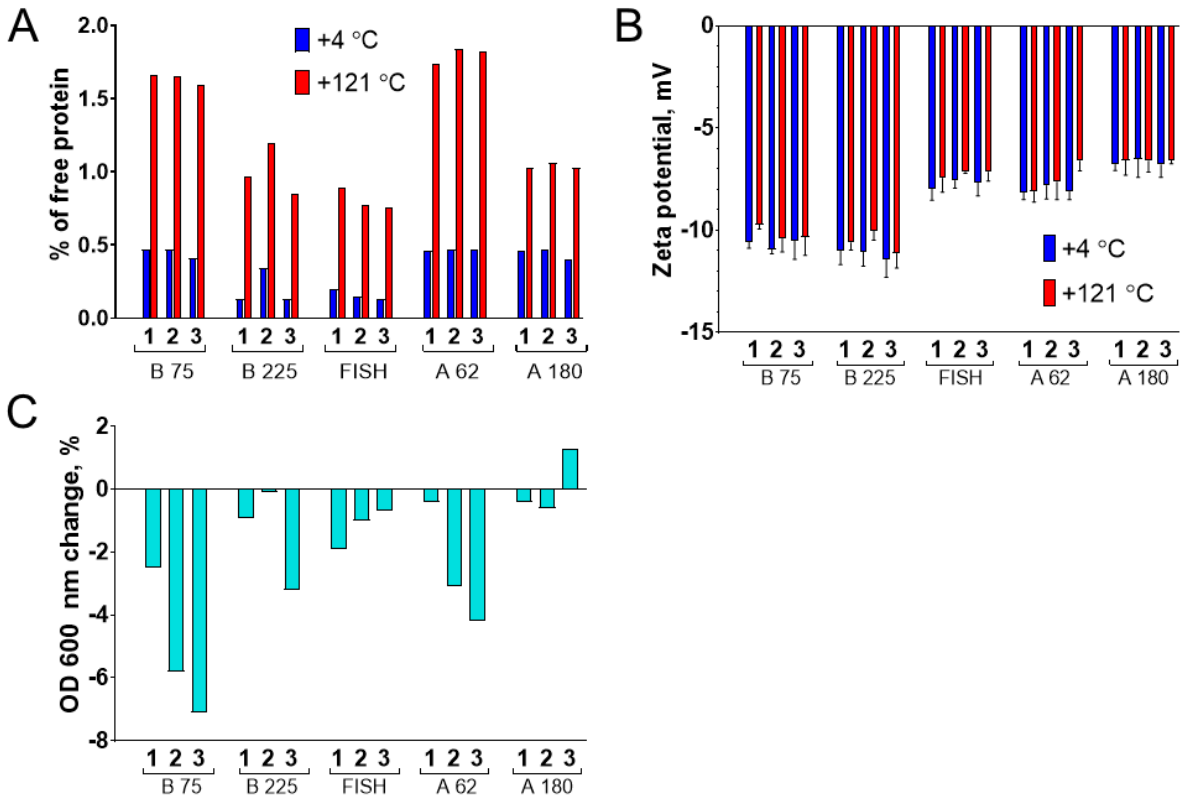

Figure 24. Properties of sterilized (+121 °C) and non-sterilized (+4 °C) nanoparticles. A - the percentage of free protein in relation to nanoparticle concentration; B - zeta potential at a pH 7; C - change of turbidity of the gelatin nanoparticle suspensions after sterilization.

The influence of autoclave sterilization on the integrity of gelatin nanoparticles was studied by two methods.

Firstly, we measured the concentration of free protein in nanoparticle suspensions before and after autoclaving. Nanoparticles were pelleted by centrifugation, and supernatants were analyzed by BCA assay. Generally, after autoclave sterilization, the percentage of free gelatin molecules did not exceed 1-2% of total nanoparticle weight, which is, though, 2-5-fold higher in comparison with untreated nanoparticles (**Figure 24A**). Partial degradation and aggregation of gelatin nanoparticles upon autoclaving are in line with previous reports (**Geh, 2018 thesis**).

Secondly, we assessed the turbidity of nanoparticles preparations. Recently, Geh with colleagues observed a pronounced decrease of turbidity after sterilization of gelatin nanoparticles in the autoclave (**Geh, 2018 thesis**). For almost all batches of nanoparticles slight (not more than 8%) decrease in turbidity was observed. Both changes in size and dissolution could affect turbidity **Figure 24C**. Taking into account DLS data and free protein change we suppose that dissolution of a small percentage of nanoparticles can take place during sterilization.

Another issue is a chemical alteration caused by sterilization. Autoclaving leads to a decrease of cross-linking degree and increase of free amino group content in gelatin nanoparticles (**Geh, 2018 thesis**). Indeed, the zeta potential of sterilized nanoparticles was a bit more positive (by 1-2 mV) compared to plain nanoparticles (**Figure 24B**). Moreover, the color of nanoparticle suspensions changed after sterilization (**Figure 26**). The formation of new chemical bonds in gelatin nanoparticles was indirectly assessed by studying their fluorescence behavior at different excitation wavelengths. We compared emission spectra of gelatin nanoparticles before and after sterilization. Excitation wavelengths varied from 260 to 560 nm. Emission spectra recorded at excitation wavelengths of 300, 400, and 500 nm are presented in the **figure 25**. Excitation at 300 and 400 nm resulted in a strong increase of emission, whereas excitation at 500 nm had almost no effect. These results confirm that some structural alterations accompanied autoclaving. Change of emission was not caused by evaporation of nanoparticle suspension, otherwise, an increase of emission should also be observed after excitation at 500 nm. Moreover, the volume of nanoparticle suspension was controlled in the course of the experiment.

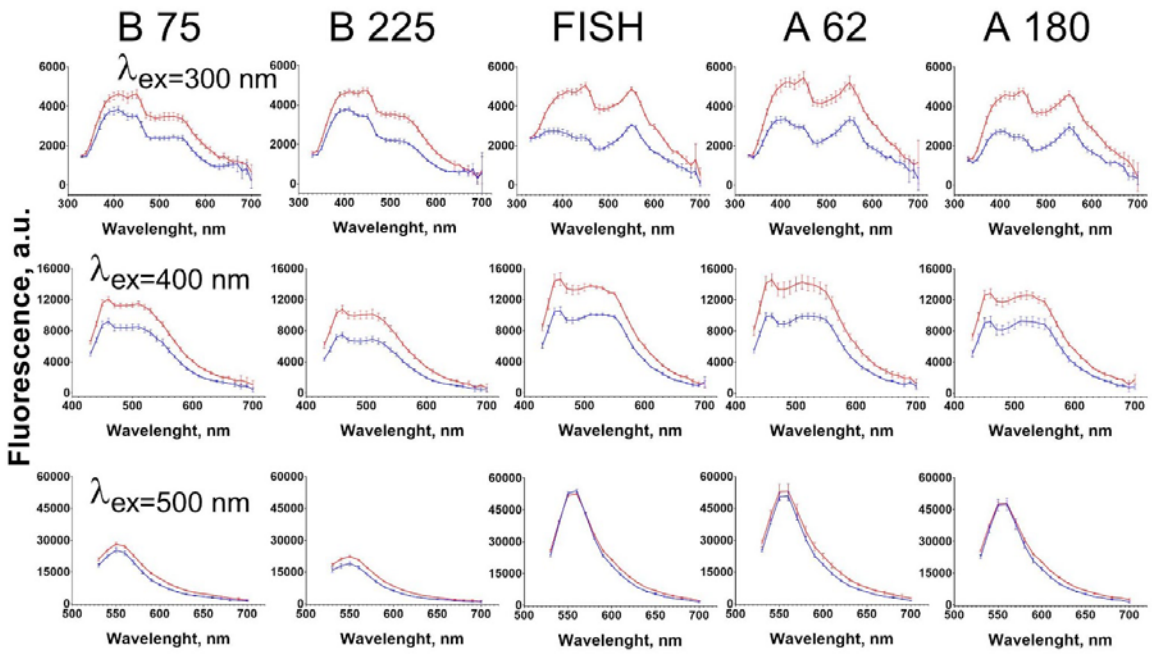

Figure 25. Emission spectra of non-autoclaved (blue) and autoclaved (red) gelatin nanoparticles at excitation wavelengths of 300 (top row), 400 (middle row), and 500 nm (bottom row).

Despite autoclaved samples retained their key properties, we should note that autoclaving of gelatin nanoparticles is appropriate mainly for food applications or in other fields which do not require parenteral usage of nanoparticles. Autoclaving kills microorganisms but does not remove endotoxin, which can interfere with cell and tissue culturing and provokes immune system activation or even endotoxin shock in animals (**Vetten, 2014**). Autoclaving may be useful for applications where the presence of a small percentage of aggregates and free protein is acceptable. For pharmaceutical purposes, the whole synthesis can be performed in aseptic conditions with endotoxin-free reagents. Another option is post-synthesis depyrogenation and sterilization by gamma-irradiation (**Monti, 2021**), which was shown to be compatible with gelatin nanoparticle formulations (**Geh, 2018**).

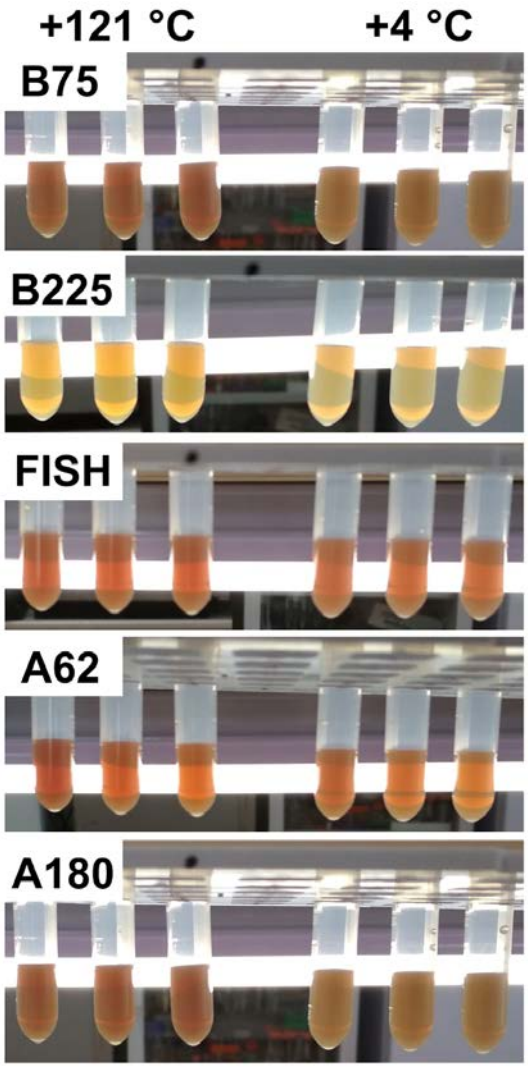

Figure 26. Color of autoclaved and non-autoclaved gelatin nanoparticle suspensions

3.8. Effect of gelatin nanoparticles on viability of peripheral blood mononuclear cells

Application of gelatin nanoparticles in drug/gene/antigen delivery or bioimaging requires their blood circulation, making interaction with blood components unavoidable. Therefore, the toxicity of gelatin nanoparticles towards blood immune cells was studied. Peripheral blood mononuclear cells (PBMC) are a complex mixture of cells with a round-shaped nucleus comprising regulatory and effector cells, namely T cells, B cells, NK cells, and monocytes. Being primary cells, they represent the reaction of human blood cells to nanoparticles in a more natural way in comparison with available lymphocyte cell lines (**Jeong, 2017**). PBMC were isolated from the blood of three healthy donors and incubated with glycine-quenched sterilized gelatin nanoparticles for 24 h. Dead cells were stained with propidium iodide and quantified by flow cytometry. The range of gelatin nanoparticles concentrations was based on literature data. The concentration of nanoparticles in the blood can reach values of hundreds of micrograms per milliliter after parenteral administration (**Ong, 2021**).

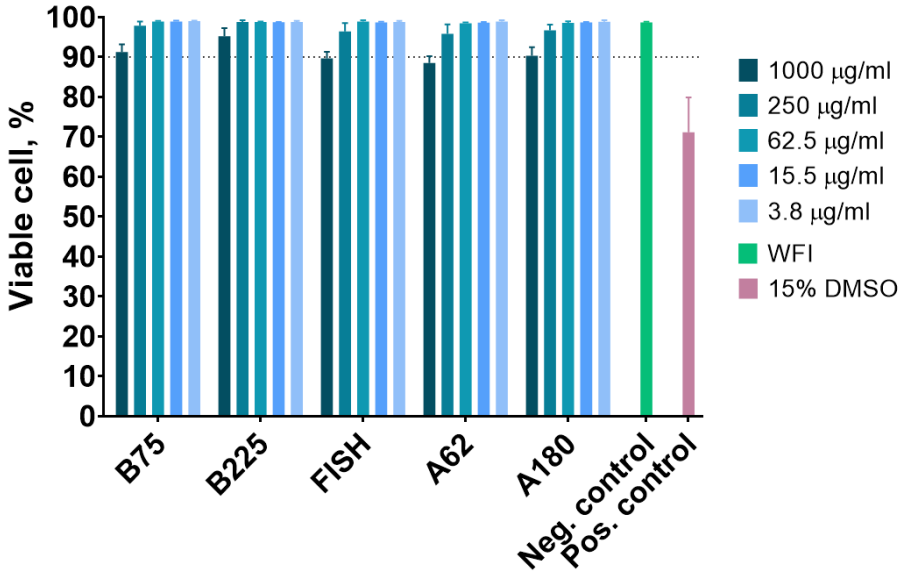

Figure 27. Viability of PBMC in the presence of various concentrations of gelatin nanoparticles. WFI - water for injection.

The viability of gelatin nanoparticles was higher than 88% in a whole range of concentrations, indicating low cytotoxicity of gelatin nanoparticles (**Figure 27**). However, we should note that nanoparticles engulfed or absorbed by cells interfere with fluorescence measurements. Nanoparticles emit fluorescence between 543 and 627 nm (**Figure S4**) (propidium iodide detection channel), moreover at higher nanoparticle concentrations PBMC uptake (or absorb) more nanoparticles as can be seen by the increase of cell granularity (which was assessed by measuring the side scattering of cells) (**Figure S5**). Therefore, a more thorough study of gelatin nanoparticle toxicity is to be made in the future.

4. Conclusion

The modified desolvation method makes it possible to synthesize nanoparticles from gelatin regardless of its origin and bloom number. This method can be a facile alternative to the commonly utilized two-step desolvation method. Noteworthy, in the course of nanoparticle synthesis, we used common laboratory equipment: centrifuge with a capacity less than 500 ml, thermostat, water bath, and sonicator. All the reagents used are readily available and cheap. Synthesis procedures are simple and can be performed even by non-trained personnel.

One can conclude that the proposed method works well in a laboratory, but is it suitable for large-scale nanoparticle manufacturing? To meet the needs of market consumers, nanoparticles manufacturing rates should be as high as kilograms per day (**A matter of scale, 2016**, **Feng, 2019**). Theoretically, this goal can be achieved by a straightforward hundredfold increase of synthesis volumes and by performing multiple parallel syntheses. Undoubtedly, volume increase can lead to a change of nanoparticles size, yield, and their properties caused by mass transfer rate alterations (**Feng, 2019**). However, we emphasized that at certain gelatin concentrations mixing rate has a very small effect on nanoparticles size. Moreover, as one can see, gelatin does not aggregate being quickly mixed with a large volume of non-solvent (in contrast to, say, bovine serum albumin). In our opinion, these factors favor the scaling-up of the proposed modified desolvation method.

Recently direct addition of non-solvent to gelatin under gentle mixing has been realized in the microfluidics-assisted method (**Van Den Broek, 2016**). This approach allows continuous manufacturing of gelatin nanoparticles. Microfluidic devices enable large-scale synthesis of nanoparticles and better control over their preparation (**Chiesa, 2018, Zhang, 2020**), however, scaling-up can be challenging as it requires chip parallelization or channel diameter increase (**Matthew, 2020**). The high costs of setting up the microfluidic devices for industrial scale-up, as well as technical issues (e.g. channels clogging (**Chiesa, 2018, Niculescu, 2021**) are among potential barriers to their implementation. Thus, despite numerous advantages of microfluidics

technology, batch methods (including modified desolvation method) are still attractive in terms of their industrial application (**Matthew, 2020**).

In this study, glutaraldehyde was utilized for nanoparticle cross-linking. Despite being effective and widely available, it raises concerns about its potential toxicity (both as a component of nanoparticles and a component of waste). Therefore, the toxicity of gelatin nanoparticles stabilized with glutaraldehyde needs to be thoroughly tested. Besides, other approaches to gelatin cross-linking should be considered e.g. reagentless irradiative cross-linking (**Varca, 2016**) or stabilization by polymer entrapment (**Khan, 2020**).

The environmental impact of all nanoparticle synthesis components should also be considered before their translation into practice (**Egorova, 2020**). The main concerns are usually related to the toxicity of cross-linking agents, however, proper management of organic waste comprising organic solvent itself and products of its interaction with the cross-linking agent can also be a problem. More cheap and effective (from the synthesis point of view) solvent can be less appropriate in terms of disposal, therefore different combinations of desolvating agents (not necessary organic solvents!) and cross-linking agents are to be tested. Here we used short-chain alcohols as desolvating agents. They can be classified as environmentally favorable solvents (**Capello, 2007**). However, other organic solvents or other approaches to desolvation (e.g. salting out), which can be potentially more effective or safe, need to be studied in the future. Moreover, testing of different cross-linking agents or non-solvents is of importance, because some substances to be loaded in gelatin nanoparticles can be incompatible with specific synthesis conditions, i.e. non-soluble in particular desolvating agent, unstable at high pH, and so on.

In conclusion, we need to mention several limitations of the present study:

1. The size of all synthesized gelatin nanoparticles exceeded 100 nm. We did not obtain smaller nanoparticles, however, the desolvation method allows the preparation of nanoparticles whose diameter is less than 100 nm (**Won, 2008, Shamarekh, 2020**). We suppose that a decrease of initial gelatin concentration or increase of gelatin solution pH is a possible way to obtain nanoparticles smaller than 100 nm.
2. We did not prepare nanoparticles from gelatin solutions with concentrations higher than 20 mg/ml at a high scale. As we mentioned in Section our goal was to prepare relatively small nanoparticles, less than 200 nm, which is possible by using smaller gelatin concentrations for all tested gelatin types. Data obtained in the course of optimization experiments and our previous results (**Khramtsov, 2021**) both demonstrate that gelatin nanoparticles can be prepared at high starting gelatin concentrations. Variation of pH and volume of the desolvating agent is a possible way to decrease the size of nanoparticles when the concentration of gelatin is high.
3. As we mentioned before, we did not remove endotoxin from gelatin nanoparticles nor examine LPS concentration in nanoparticle preparations prior to cell viability testing. Synthesis of apyrogenic nanoparticles is a challenging task, which requires a separate set of experiments and was, therefore, beyond the scope of the present work. We just note that the protocol of gelatin depyrogenation was previously reported by Singh et al. (**Singh, 2016**), besides post-synthesis depyrogenation by gamma-irradiation also remains a possible option (**Monti, 2021**).
4. The effect of several factors on the desolvation process was not studied: temperature of starting materials (**Azarmi, 2006**), salt concentration, acidic pH values, gelatin pre-incubation (**Vinjamuri, 2021**), the longevity of incubation with alcohols, and so on. Nevertheless, we performed preliminary experiments adding NaCl before desolvation. The addition of salt resulted in the formation of microparticles visible by the eye, however, a systematic study has not been conducted.
5. Despite various types of animal gelatin being tested, we did not prepare nanoparticles from human recombinant gelatin. Application of natural gelatin from animal sources can be limited due to pathogen (first of all, prions) contamination, religious reasons, and its potential immunogenicity (**Alipal, 2021**). In previous papers, gelatin nanoparticles synthesized from recombinant human gelatin by one-step desolvation method were described (**Won, 2008**), therefore we believe that the universal nature of the proposed method enables usage of human recombinant gelatin as a starting material.

Supplementary Materials

Figure S1: size of gelatin nanoparticles; Figure S2: yield of gelatin nanoparticles; Figure S3: emission spectra of gelatin nanoparticles; Figure S4: interference of nanoparticle fluorescence with propidium iodide staining; Figure S5: side scattering of PBMC; Table S1: literature data on yields of desolvation and nanoprecipitation methods.

Author Contributions: Pavel Khramtsov: Formal analysis, Investigation, Visualization, Writing - original draft. Oksana Burdina: Formal analysis, Investigation. Sergey Lazarev: Investigation. Anastasia Novokshonova: Investigation. Maria Bochkova: Investigation. Valeria Timganova: Investigation. Dmitriy Kiselkov: Investigation. Svetlana Zamorina: Resources, Conceptualization, Writing - review & editing. Mikhail Rayev: Conceptualization, Resources, Funding acquisition, Writing - review & editing.

Funding: The reported study was funded by RFBR and Kaliningrad Oblast according to the research project № 19-415-393005 (preparation of fluorescence gelatin nanoparticles and study of their fluorescent properties), by RFBR research project 19-015-00408 (preparation of gelatin nanoparticles by the desolvation method), and by Research Program No.AAAA-A19-119112290010-7 (assessment of nanoparticles cytotoxicity).

Institutional Review Board Statement: Research was approved by the Review Board of the Institute of Ecology and Genetics of Microorganisms UB RAS (IRB00010009).

Informed Consent Statement: All procedures were performed in accordance with the 1964 Declaration of Helsinki and its later amendments or comparable ethical standards. Written informed consent was obtained from all volunteers.

Data Availability Statement: The datasets used and/or analyzed during the current study are available from the corresponding author on reasonable request.

Conflicts of Interest: The authors declare that they have no conflict of interest.

References

A matter of scale. *Nat. Nanotechnol.* **2016**, *11*, 733. DOI: 10.1038/nnano.2016.180

Abdelrady, H., Hathout, R. M., Osman, R., Saleem, I., Mortada, N. D. Exploiting gelatin nanocarriers in the pulmonary delivery of methotrexate for lung cancer therapy. *Eur. J. Pharm. Sci.* **2019**, *133*, 115-126. DOI: 10.1016/j.ejps.2019.03.016

Ahlers, M., Coester, C., Zwiorek, K., Zillies, J. Nanoparticles and method for the production thereof. Patent WO2006021367A1. 2005.

Ahsan, S. M., Rao, C. M. The role of surface charge in the desolvation process of gelatin: implications in nanoparticle synthesis and modulation of drug release. *Int. J. Nanomed.* **2017**, *12*, 795–808. DOI: 10.2147/IJN.S124938

Alipal, J., Mohd Pu'ad, N., Lee, T.C. Nayan, N., Sahari, N., Basri, H., Idris, M., Abdullah, H. A review of gelatin: Properties, sources, process, applications, and commercialisation. *Mater. Today: Proc.* **2021**, *42*. 240-250. DOI: 10.1016/j.matpr.2020.12.922.

Arroyo-Maya, I.J., Rodiles-López, J.O., Cornejo-Mazón, M., Gutiérrez-López, G.F., Hernández-Arana, A., Toledo-Núñez, C., Barbosa-Cánovas, G.V., Flores-Flores, J.O., Hernández-Sánchez, H. Effect of different treatments on the ability of α-lactalbumin to form nanoparticles. *J. Dairy Sci.* **2012**, *95*, 6204-6214. DOI: 10.3168/jds.2011-5103

Azarmi, S., Huang, Y., Chen, H., McQuarrie, S., Abrams, D., Roa, W., Finlay, W. H., Miller, G. G., & Löbenberg, R. Optimization of a two-step desolvation method for preparing gelatin nanoparticles and cell uptake studies in 143B osteosarcoma cancer cells. *J. Pharm. Pharm. Sci.* **2006**, *9*,124–132.

Balthasar, S. Charakterisierung proteinbasierter Nanopartikel zum Transport von Oligonukleotiden für eine Rezeptor-vermittelte Zellaufnahme. Dissertation zur Erlangung des Doktorgrades der Naturwissenschaften. 2005. Available online: http://d-nb.info/978388593/34 (accessed on 15 July 2021).

Balthasar, S., Michaelis, K., Dinauer, N., Von Briesen, H., Kreuter, J., Langer, K. Preparation and characterisation of antibody modified gelatin nanoparticles as drug carrier system for uptake in lymphocytes. *Biomaterials* **2005**, *26*, 2723-2732. DOI: 10.1016/j.biomaterials.2004.07.047

Bello, A.B., Kim, D., Kim, D., Park, H., Lee, S.-H. Engineering and functionalization of gelatin biomaterials: From cell culture to medical applications. *Tissue Eng., Part B* **2020**, *26*, 164-180. DOI: 10.1089/ten.teb.2019.0256

Beyer, C., Claisen, L. Ueber die Einführung von Säureradicalen in Ketone. *Ber. Dtsch. Chem. Ges*. **1887**, *20*, 2178

Cai, B., Rao, L., Ji, X., Bu, L. L., He, Z., Wan, D., Yang, Y., Liu, W., Guo, S., Zhao, X. Z. Autofluorescent gelatin nanoparticles as imaging probes to monitor matrix metalloproteinase metabolism of cancer cells. *J. Biomed. Mater. Res., Part A* **2016**, *104*, 2854–2860. DOI: 10.1002/jbm.a.35823

Capello, C., Fischer, U., Hungerbühler, K. What is a green solvent? A comprehensive framework for the environmental assessment of solvents. *Green Chem*. **2007**, *9*, 927. DOI: 10.1039/b617536h

Chiesa, E., Dorati, R., Pisani, S., Conti, B., Bergamini, G., Modena, T., & Genta, I. The Microfluidic Technique and the Manufacturing of Polysaccharide Nanoparticles. *Pharmaceutics* **2018**, *10*, 267. DOI: 10.3390/pharmaceutics10040267

Clark, C.C., Aleman, J., Mutkus, L., Skardal, A. A mechanically robust thixotropic collagen and hyaluronic acid bioink supplemented with gelatin nanoparticles. *Bioprinting* **2019**, *16*, e00058. DOI: 10.1016/j.bprint.2019.e00058

Coester C.J., Langer K., van Briesen H., Kreuter J. Gelatin nanoparticles by two step desolvation--a new preparation method, surface modifications and cell uptake. *J. Microencapsulation* **2000**, *17*, 187-193. DOI: 10.1080/026520400288427

Das R.P., Chakravarti S., Patel S.S., Lakhamje P., Gurjar M., Gota V., Singh B.G., Kunwar A. Tuning the pharmacokinetics and efficacy of irinotecan (IRI) loaded gelatin nanoparticles through folate conjugation. *Int J Pharm.* **2020** *586*, 119522. DOI: 10.1016/j.ijpharm.2020.119522.

de Abreu Costa, L., Henrique Fernandes Ottoni, M., Dos Santos, M. G., Meireles, A. B., Gomes de Almeida, V., de Fátima Pereira, W., Alves de Avelar-Freitas, B., Eustáquio Alvim Brito-Melo, G. Dimethyl Sulfoxide (DMSO) Decreases Cell Proliferation and TNF-α, IFN-γ, and IL-2 Cytokines Production in Cultures of Peripheral Blood Lymphocytes. *Molecules* **2017**, *22*, 1789. DOI: 10.3390/molecules22111789

Derkach, S.R., Voron'ko, N.G., Kuchina, Y.A., Kolotova, D.S. Modified Fish Gelatin as an Alternative to Mammalian Gelatin in Modern Food Technologies. *Polymers* **2020**, *12*, 3051. DOI: 10.3390/polym12123051

Diba, M., Koons, G.L., Bedell, M.L., Mikos, A.G. 3D printed colloidal biomaterials based on photo-reactive gelatin nanoparticles. *Biomaterials*, **2021**, *274*, 120871. DOI: 10.1016/j.biomaterials.2021.120871

Ding, M., Zhang, T., Zhang, H., Tao, N., Wang, X., Zhong, J. Effect of preparation factors and storage temperature on fish oil-loaded crosslinked gelatin nanoparticle pickering emulsions in liquid forms. *Food Hydrocolloids* **2019**, *95*, 326-335. DOI: 10.1016/j.foodhyd.2019.04.052

Egorova, K.S., Galushko, A.S., Ananikov, V.P. Introducing tox-Profiles of Chemical Reactions. *Angew. Chem., Int. Ed. Engl.* **2020**, *59*, :22296-22305. DOI: 10.1002/anie.202003082.

El-Sayed, N., Trouillet, V., Clasen, A., Jung, G., Hollemeyer, K., Schneider, M., NIR-Emitting Gold Nanoclusters–Modified Gelatin Nanoparticles as a Bioimaging Agent in Tissue. *Adv. Healthcare Mater*. **2019**, *8*, 1900993. DOI: 10.1002/adhm.201900993

Esteban-Pérez, S., Andrés-Guerrero, V., López-Cano, J.J., Molina-Martínez, I., Herrero-Vanrell, R., Bravo-Osuna, I. Gelatin Nanoparticles-HPMC Hybrid System for Effective Ocular Topical Administration of Antihypertensive Agents. *Pharmaceutics* **2020**, *12*, 306. DOI: 10.3390/pharmaceutics12040306

Farrugia, C. A., Groves, M. J. Gelatin Behaviour in Dilute Aqueous Solution: Designing a Nanoparticulate Formulation. *J. Pharm. Pharmacol.* **1999**, *51*, 643–649. DOI: 10.1211/0022357991772925

Feng, J., Markwalter, C. E., Tian, C., Armstrong, M., Prud'homme, R. K. Translational formulation of nanoparticle therapeutics from laboratory discovery to clinical scale. *J. Transl. Med.* **2019**, *17*, 200. DOI: 10.1186/s12967-019-1945-9

Feng, X., Dai, H., Ma, L., Fu, Y., Yu, Y., Zhou, H., Guo, T., Zhu, H., Wang, H., Zhang, Y. Properties of Pickering emulsion stabilized by food-grade gelatin nanoparticles: influence of the nanoparticles concentration. *Colloids Surf., B* **2020**, *196*, 111294. DOI: 10.1016/j.colsurfb.2020.111294

Fuchs, S. Gelatin Nanoparticles as a modern platform for drug delivery: formulation development and immunotherapeutic strategies. Dissertation. Ludwig Maximilian University of Munich. Munich. 29. July 2010.

Geh K.J., Hubert M., Winter G. Progress in formulation development and sterilisation of freeze-dried oligodeoxynucleotide-loaded gelatine nanoparticles. *Eur J Pharm Biopharm.* **2018**, *129*, 10-20. DOI: 10.1016/j.ejpb.2018.05.016

Geh, K. Gelatine nanoparticles as immunomodulatory drug delivery system: advanced production processes and clinical trials. Dissertation. Ludwig Maximilian University of Munich. Munich. 16 March 2018. DOI: 10.5282/edoc.22033

Geh, K. J., Hubert, M., Winter, G. Optimisation of one-step desolvation and scale-up of gelatine nanoparticle production. *J. Microencapsulation*, **2016**, *33*, 595–604. DOI: 10.1080/02652048.2016.1228706

Gomez-Guillen, M.C., Gimenez, B., Lopez-Caballero, M.E., Montero, M.P. Functional and bioactive properties of collagen and gelatin from alternative sources: A review. *Food Hydrocolloids* **2011**, *25*, 1813-1827. DOI: 10.1016/j.foodhyd.2011.02.007

Hsieh, P., Segal, R., Chen, L. B. Studies of fibronectin matrices in living cells with fluoresceinated gelatin. *J. Cell Biol.*, **1980**, *87*, 14–22. DOI: 10.1083/jcb.87.1.14

Jeong, H., Hwang, J., Lee, H., Hammond, P. T., Choi, J., Hong, J. In vitro blood cell viability profiling of polymers used in molecular assembly. *Sci. Rep*. **2017**, *7*, 9481. DOI: 10.1038/s41598-017-10169-5

Kaul, G., Amiji, M. Long-circulating poly(ethylene glycol)-modified gelatin nanoparticles for intracellular delivery. *Pharm. Res*. **2002**, *19*, 1061-1067. DOI: 10.1023/A:1016486910719

Khan S. A. Mini-Review: Opportunities and challenges in the techniques used for preparation of gelatin nanoparticles. *Pak. J. Pharm. Sci.* **2020**, *33*, 221–228.

Khan, S. A., Ali, H., Ihsan, A., Sabir, N. Tuning the size of gelatin nanoparticles produced by nanoprecipitation. *Colloid J.* **2015**, *77*, 672–676. DOI: 10.1134/s1061933x15050105

Khramtsov P., Kalashnikova T., Bochkova M., Kropaneva M., Timganova V., Zamorina S., Rayev M. Measuring the concentration of protein nanoparticles synthesized by desolvation method: Comparison of Bradford assay, BCA assay, hydrolysis/UV spectroscopy and gravimetric analysis. *Int J Pharm.* **2021**, *15*, 120422. DOI: 10.1016/j.ijpharm.2021.120422

Klier, J., Bartl, C., Geuder, S., Geh, K.J., Reese, S., Goehring, L.S., Winter, G., Gehlen, H. Immunomodulatory asthma therapy in the equine animal model: A dose-response study and evaluation of a long-term effect. *Immun., Inflammation Dis.* **2019**, *7*, 130-149. DOI: 10.1002/iid3.252

Kommareddy, S., Amiji, M. M. Preparation and Loading of Gelatin Nanoparticles. *Cold Spring Harbor Protocols*, **2008**, *2*, pdb.prot4885–pdb.prot4885. DOI: 10.1101/pdb.prot4885

Langer, K., Anhorn, M. G., Steinhauser, I., Dreis, S., Celebi, D., Schrickel, N., Faust, S., Vogel, V. Human serum albumin (HSA) nanoparticles: reproducibility of preparation process and kinetics of enzymatic degradation. *Int. J. Pharm*. **2008** *347*, 109–117. DOI: 10.1016/j.ijpharm.2007.06.028

Langevin, D., Raspaud, E., Mariot, S., Knyazev, A., Stocco, A., Salonen, A., Luch, A., Haase, A., Trouiller, B., Relier, C., Lozano, O., Thomas, S., Salvati, A., Dawson, K. Towards reproducible measurement of nanoparticle size using dynamic light scattering: Important controls and considerations. *NanoImpact* **2018**, *10*, 161–167. DOI: 10.1016/j.impact.2018.04.002

Lee, E. J., Khan, S. A., Park, J. K., Lim, K.-H. Studies on the characteristics of drug-loaded gelatin nanoparticles prepared by nanoprecipitation. *Bioprocess Biosyst. Eng.* **2011**, *35*, 297–307. DOI: 10.1007/s00449-011-0591-2

Leo, E., Vandelli, M.A., Cameroni, R., Forni, F. Doxorubicin-loaded gelatin nanoparticles stabilized by glutaraldehyde: Involvement of the drug in the cross-linking process. *Int J Pharm.* **1997***, 155*, 75-82. DOI: 10.1016/S0378-5173(97)00149-X

Lin, A., Liu, Y., Zhu, X., Chen, X., Liu, J., Zhou, Y., Qin, X., Liu, J. Bacteria-Responsive Biomimetic Selenium Nanosystem for Multidrug-Resistant Bacterial Infection Detection and Inhibition. *ACS Nano* **2019**, *13*, 13965-13984. DOI: 10.1021/acsnano.9b05766

Lowry, G.V., Hill, R.J., Harper, S., Rawle, A.F., Hendren, C.O., Klaessig, F., Nobbmann, U., Sayre, P., Rumble, J. Guidance to improve the scientific value of zeta-potential measurements in nanoEHS. *Environ. Sci.: Nano* **2016**, *3*, 953-965. DOI: 10.1039/c6en00136j

Lu, Z., Yeh, T.-K., Tsai, M., Au, J.L.-S., Wientjes, M.G. Paclitaxel-loaded gelatin nanoparticles for intravesical bladder cancer therapy. *Clin. Cancer Res.* **2004**, *10*, 7677-7684. DOI: 10.1158/1078-0432.CCR-04-1443

Ma, X., Hargrove, D., Dong, Q., Song, D., Chen, J., Wang, S., Lu, X., Cho, Y.K., Fan, T.-H., Lei, Y. Novel green and red autofluorescent protein nanoparticles for cell imaging and in vivo biodegradation imaging and modeling. *RSC Adv*. **2016**, *6*, 50091–50099. DOI: 10.1039/c6ra06783b

Madkhali, O. Cationic Gelatin/Pluronic-based Nanoparticles as Novel Non-Viral Delivery Systems for Gene Therapy. Ph.D. thesis. University of Waterloo, Ontario. 2018.

Matthew S.A.L., Totten J.D., Phuagkhaopong S., Egan G., Witte K., Perrie Y., Seib F.P. Silk Nanoparticle Manufacture in Semi-Batch Format. *ACS Biomater. Sci. Eng.* **2020** *14*, 6748-6759. DOI: 10.1021/acsbiomaterials.0c01028

Mehravar R., Jahanshahi R., Najafpour G.D., Saghatoleslami N. Applying the Taguchi method for optimized fabrication of α-lactalbumin nanoparticles as carrier in drug delivery and food science. *Iranica J. Energy Environ.* **2011**, *2*, 87-91

Mironov L. Y., Parfenov P. S., Shurukhina A. V., Lebedev Y. I., Metlenko A. A. Delayed Fluorescence of Dyes Sensitized by Eu^{3+} Chelate Nanoparticles. *J. Phys. Chem. C*. **2017**, *121*, 19958-19965. DOI: 10.1021/acs.jpcc.7b03648

Mohammad-Beigi, H., Shojaosadati, S. A., Morshedi, D., Mirzazadeh, N., Arpanaei, A. The Effects of Organic Solvents on the Physicochemical Properties of Human Serum Albumin Nanoparticles. *Iran. J. Biotechnol*. **2016**, *14*, 45–50. DOI: 10.15171/ijb.1168

Monti, F., Manfredi, G., Palamà, I. E., Kovtun, A., Zangoli, M., D'Amone, S., Ortolani, L., Bondelli, G., Szreder, T., Bobrowski, K., D'Angelantonio, M., Lanzani, G., Di, F., Sterilization of Semiconductive Nanomaterials: The Case of Water-Suspended Poly-3-Hexylthiophene Nanoparticles. *Adv. Healthcare Mater.* **2021**, *10*, 2001306. DOI: 10.1002/adhm.202001306

Morel, M.-H., Redl, A., Guilbert, S. Mechanism of Heat and Shear Mediated Aggregation of Wheat Gluten Protein upon Mixing. *Biomacromolecules* **2002**, *3*, 488–497. DOI: 10.1021/bm015639p

Narayanan, D, Geena, M. G., Lakshmi, H., Koyakutty, M., Nair, S., Menon, D. Poly-(ethylene glycol) modified gelatin nanoparticles for sustained delivery of the anti-inflammatory drug Ibuprofen-Sodium: an in vitro and in vivo analysis. *Nanomedicin*e **2013**, *9*, 818-28. DOI: 10.1016/j.nano.2013.02.001.

Niculescu, A.-G.; Chircov, C.; Bîrcˇa, A.C.; Grumezescu, A.M. Nanomaterials Synthesis through Microfluidic Methods: An Updated Overview. *Nanomaterials* **2021**, *11*, 864. DOI: 10.3390/nano11040864

Nixon, J. R., Khalil, S. A. H., Carless, J. E. Phase relationships in the simple coacervating system isoelectric gelatin: ethanol: water. *J. Pharm. Pharmacol.* **1966**, *18*, 409–416. DOI: 10.1111/j.2042-7158.1966.tb07900.x

Ofokansi, K., Winter, G., Fricker, G., Coester, C. Matrix-loaded biodegradable gelatin nanoparticles as new approach to improve drug loading and delivery. *Eur J Pharm Biopharm.* **2010**, *76*, 1–9. DOI: 10.1016/j.ejpb.2010.04.008

Ong, Y. R., De, R., Johnston, A. P. R., In Vivo Quantification of Nanoparticle Association with Immune Cell Subsets in Blood. *Adv. Healthcare Mater.* **2021**, *10*, 2002160. DOI: 10.1002/adhm.202002160

Pei, Y., Zheng, Y., Li, Z., Liu, J., Zheng, X., Tang, K., Kaplan, D.L. Ethanol-induced coacervation in aqueous gelatin solution for constructing nanospheres and networks: Morphology, dynamics and thermal sensitivity. *J. Colloid Interface Sci*. **2021**, *582*, 610-618. DOI: 10.1016/j.jcis.2020.08.068

Saxena, A., Sachin, K., Bohidar, H. B., Verma, A. K. Effect of molecular weight heterogeneity on drug encapsulation efficiency of gelatin nano-particles. *Colloids Surf., B* **2005**, *45*, 42–48. DOI: 10.1016/j.colsurfb.2005.07.005

Seib, F. P., Jones, G. T., Rnjak-Kovacina, J., Lin, Y., Kaplan, D. L. pH-dependent anticancer drug release from silk nanoparticles. *Adv. Healthcare Mater.* **2013**, *2*, 1606–1611. DOI: 10.1002/adhm.201300034

Shamarekh, K. S., Gad, H. A., Soliman, M. E., Sammour, O. A. Towards the production of monodisperse gelatin nanoparticles by modified one step desolvation technique. *J. Pharm. Invest.* **2020**, *50*, 189–200. DOI: 10.1007/s40005-019-00455-x

Shilpi, D., Kushwah, V., Agrawal, A. K., Jain, S. Improved Stability and Enhanced Oral Bioavailability of Atorvastatin Loaded Stearic Acid Modified Gelatin Nanoparticles. *Pharm. Res.* **2017**, *34*, 1505–1516. DOI: 10.1007/s11095-017-2173-8

Shin, H., Kwak, M., Lee, T.G., Lee, J.Y. Quantifying the level of nanoparticle uptake in mammalian cells using flow cytometry. *Nanoscale* **2020**, *12*, 15743-15751. DOI: 10.1039/d0nr01627f

Singh, A., Xu, J., Mattheolabakis, G., Amiji, M. EGFR-targeted gelatin nanoparticles for systemic administration of gemcitabine in an orthotopic pancreatic cancer model. *Nanomedicine: Nanotechnology, Biology, and Medicine*, **2016**, *12*, 589–600. DOI: 10.1016/j.nano.2015.11.010

Singh, S.K., Singh, M.K., Nayak, M.K., Kumari, S., Grácio, J.J.A., Dash, D. Size distribution analysis and physical/fluorescence characterization of graphene oxide sheets by flow cytometry. *Carbon* **2011**, *49*, 684-692. DOI: 10.1016/j.carbon.2010.10.020

Sivera, M., Kvitek, L., Soukupova, J., Panacek, A., Prucek, R., Vecerova, R., Zboril, R. Silver nanoparticles modified by gelatin with extraordinary pH stability and long-term antibacterial activity. *PloS One* **2014**, *9*, e103675. DOI: 10.1371/journal.pone.0103675

Spoljaric, S., Ju, Y., Caruso, F. Protocols for Reproducible, Increased-Scale Synthesis of Engineered ParticlesBridging the “Upscaling Gap”. *Chem. Mater.* **2021**, *33*, 1099–1115 DOI: 10.1021/acs.chemmater.0c04634

Stevenson, A. T., Lewis, S. A., Whittington, A. R. Filtration initiated selective homogeneity (FISH) desolvation: A new method to prepare gelatin nanoparticles with high physicochemical consistency. *Food Hydrocolloids* **2018**, *84*, 337–342. DOI: 10.1016/j.foodhyd.2018.06.008

Subara, D., Jaswir, I., Alkhatib, M.F.R., Noorbatcha, I.A Synthesis of fish gelatin nanoparticles and their application for the drug delivery based on response surface methodology. *Adv. Nat. Sci.: Nanosci. Nanotechnol*. **2018**, *9*, 045014. DOI: 10.1088/2043-6254/aae988

Sudheesh, M. S., Vyas, S. P., Kohli, D. V. Nanoparticle-based immunopotentiation via tetanus toxoid-loaded gelatin and aminated gelatin nanoparticles. *Drug Delivery* **2011**, *18*, 320–330. DOI: 10.3109/10717544.2010.549525

Sun, S., Xiao, Q.-R., Wang, Y., & Jiang, Y. Roles of alcohol desolvating agents on the size control of bovine serum albumin nanoparticles in drug delivery system. *J. Drug Delivery Sci. Technol.* **2018**, *47*, 193–199. DOI: 10.1016/j.jddst.2018.07.018

Tsai, Y.-J., Hu, C.-C., Chu, C.-C., Imae, T. Intrinsically fluorescent PAMAM dendrimer as gene carrier and nanoprobe for nucleic acids delivery: Bioimaging and transfection study. *Biomacromolecules* **2011**, *12*, 4283-4290. DOI: 10.1021/bm201196p

Tyllianakis, P.E., Kakabakos, S.E., Evangelatos, G.P., Ithakissios, D.S. Direct colorimetric determination of solid-supported functional groups and ligands using bicinchoninic acid. *Anal. Biochem*. **1994**, *219*, 335-340. DOI: 10.1006/abio.1994.1273

Van Den Broek, S. Nieuwland, P.J. Kaspar Koch, K. Continuous flow production of gelatin nanoparticles. US Patent. US9289499B2. 2016.

Vandervoort J, Ludwig A. Preparation and evaluation of drug-loaded gelatin nanoparticles for topical ophthalmic use. *Eur. J. Pharm. Biopharm*. **2004**, *57*, 251-61. DOI: 10.1016/S0939-6411(03)00187-5

Varca, G.H.C., Queiroz, R.G., Lugão, A.B. Irradiation as an alternative route for protein crosslinking: Cosolvent free BSA nanoparticles. *Radiat. Phys. Chem*. **2016**, *124*, 111-115. DOI: 10.1016/j.radphyschem.2016.01.02

Vetten M.A., Yah C.S., Singh T., Gulumian M. Challenges facing sterilization and depyrogenation of nanoparticles: effects on structural stability and biomedical applications. *Nanomedicine: Nanotechnology, Biology, and Medicine* **2014**, *10*, 1391-1399. DOI: 10.1016/j.nano.2014.03.017.

Vinjamuri, B.P., Papachrisanthou, K., Haware, R.V., Chougule, M.B. Gelatin solution pH and incubation time influences the size of the nanoparticles engineered by desolvation. *J. Drug Delivery Sci. Technol.* **2021***, 63*, 102423. DOI: 10.1016/j.jddst.2021.102423

von Storp, B., Engel, A., Boeker, A., Ploeger, M., & Langer, K. Albumin nanoparticles with predictable size by desolvation procedure. *J. Microencapsulation* **2012**, *29*, 138–146. DOI: 10.3109/02652048.2011.635218

Weber, C., Coester, C., Kreuter, J., Langer, K. Desolvation process and surface characterisation of protein nanoparticles. *Int. J. Pharm*. **2000**, *194*, 91–102. DOI: 10.1016/s0378-5173(99)00370-1

Wei, W., Wang, L.-Y., Yuan, L., Wei, Q., Yang, X.-D., Su, Z.-G., Ma, G.-H. Preparation and Application of Novel Microspheres Possessing Autofluorescent Properties. *Adv. Funct. Mater.* **2007**, *17*, 3153–3158. DOI: 10.1002/adfm.200700274

Wei, X., Chen, K., Wang, Z., Huang, B., Wang, Y., Yu, M., Liu, W., Guo, S.-S., Zhao, X.-Z. Multifunctional Gelatin Nanoparticle Integrated Microchip for Enhanced Capture, Release, and Analysis of Circulating Tumor Cells. *Part. Part. Syst. Charact*. **2019**, *36*, 1900076. DOI: 10.1002/ppsc.201900076

Won, Y.-W., Kim, Y.-H. Recombinant human gelatin nanoparticles as a protein drug carrier. *J. Controlled Release* **2008**, *127*, 154–161. DOI: 10.1016/j.jconrel.2008.01.010

Yoshikawa, H., Hirano, A., Arakawa, T., Shiraki, K. Effects of alcohol on the solubility and structure of native and disulfide-modified bovine serum albumin. *Int. J. Biol. Macromol.* **2012**, *50*, 1286-1291. DOI: 10.1016/j.ijbiomac.2012.03.014

Zhang, L., Chen, Q., Ma, Y., Sun, J. Microfluidic Methods for Fabrication and Engineering of Nanoparticle Drug Delivery Systems. *ACS Appl. Bio Mater.* **2020**, *3*, 107–120 DOI: 10.1021/acsabm.9b00853

Zwiorek, K. Gelatin Nanoparticles as Delivery System for Nucleotide-Based Drugs. Dissertation. Ludwig Maximilian University of Munich. Munich. 3 August 2006

Supplementary materials

Modified desolvation method enables simple one-step gelatin nanoparticle synthesis from different gelatin types with any bloom numbers

Pavel Khramtsov[1,2,3], Oksana Burdina[2], Sergey Lazarev[2], Anastasia Novokshonova[2], Maria Bochkova[1,2], Valeria Timganova[1], Dmitriy Kiselkov[4], Svetlana Zamorina[1,2], Mikhail Rayev[1,2]*

[1]Institute of Ecology and Genetics of Microorganisms, Perm Federal Research Center of the Ural Branch of the Russian Academy of Sciences, 614081, 13 Golev st., Perm, Russia

[2]Department of Biology, Perm State University, 614068, 15 Bukirev st., Perm, Russia

[3]Center for Immunology and Cellular Biotechnology, Immanuel Kant Baltic Federal University, 236016, 14 A. Nevski st., Kaliningrad, Russia

[4]Institute of Technical Chemistry, Perm Federal Research Center of the Ural Branch of the Russian Academy of Sciences, 614013, 3 Academician Korolev st., Perm, Russia

**Corresponding author: e-mail: khramtsovpavel@yandex.ru, phone: +7 (342) 2807794, 614081, 13 Golev st., Perm, Russia*

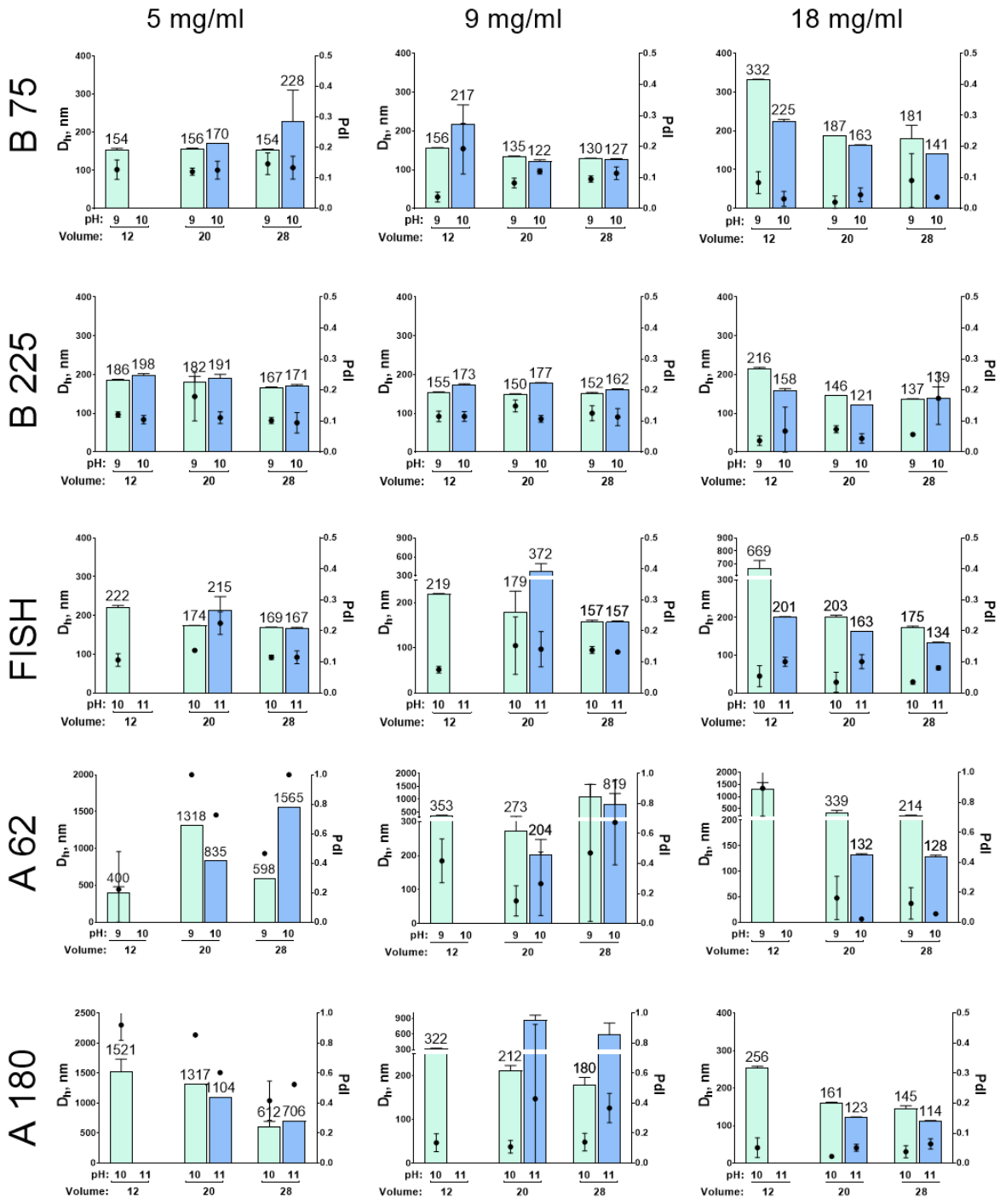

Figure S1. Size of gelatin nanoparticles prepared at different conditions using ethanol as a poor solvent. Initial gelatin concentrations are given at the top of the figure. No bar means that nanoparticles were nor formed. D_h - hydrodynamic diameter, PdI - polydispersity index.

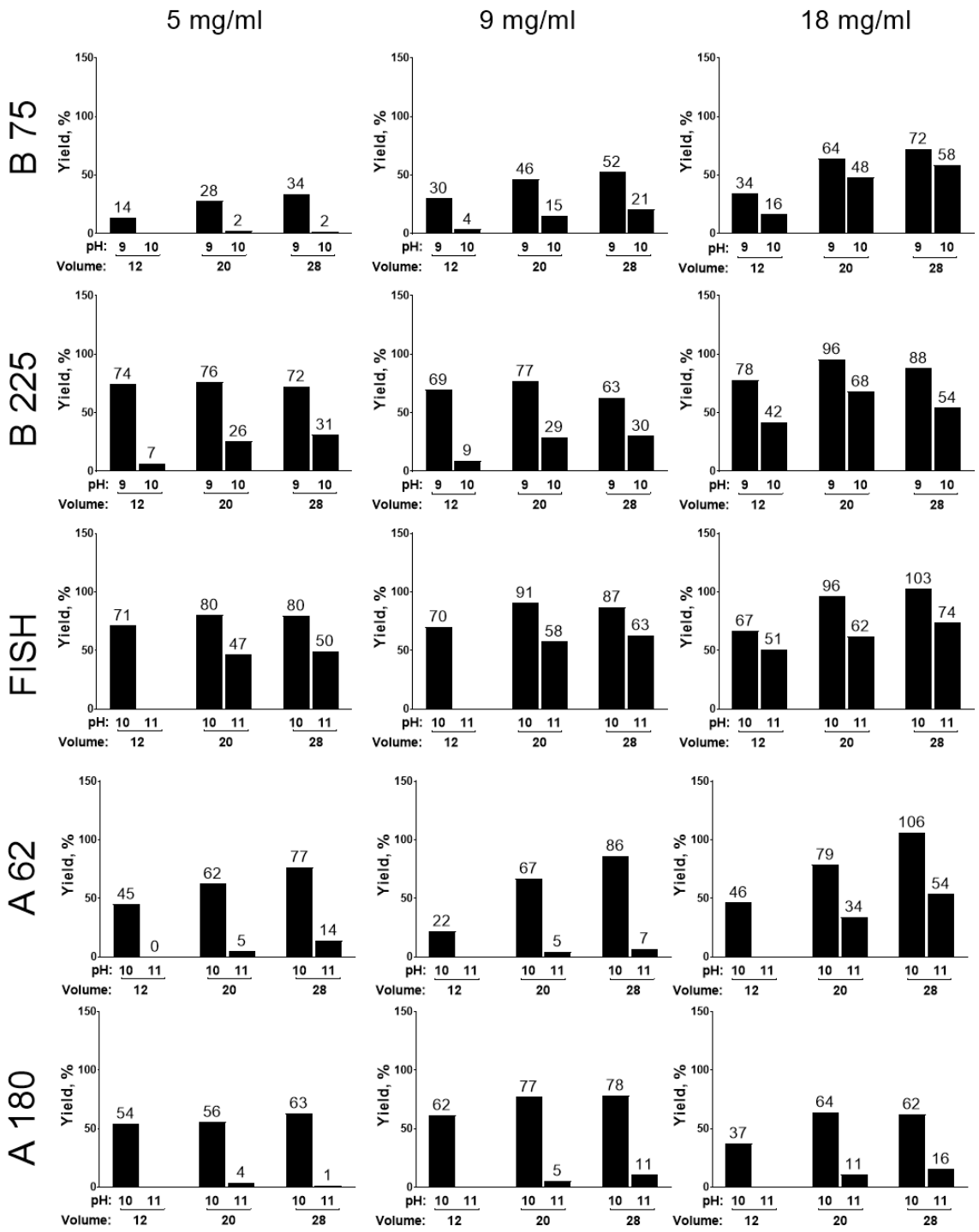

Figure S2. Yield of gelatin nanoparticles prepared at different conditions using ethanol as a poor solvent. Initial gelatin concentrations are given at the top of the figure. No bar means that nanoparticles were nor formed.

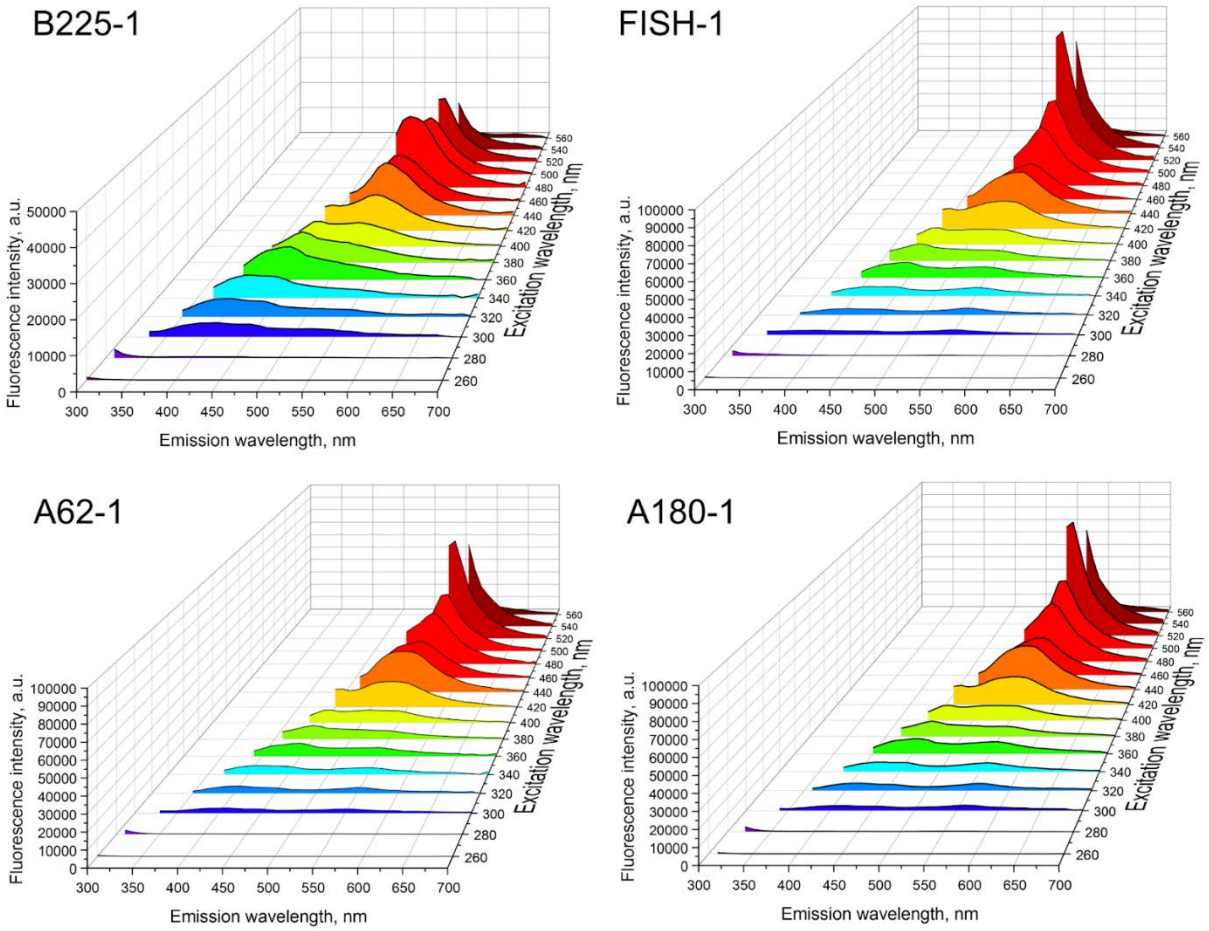

Figure S3. Emission spectra of gelatin nanoparticles at various excitation wavelengths.

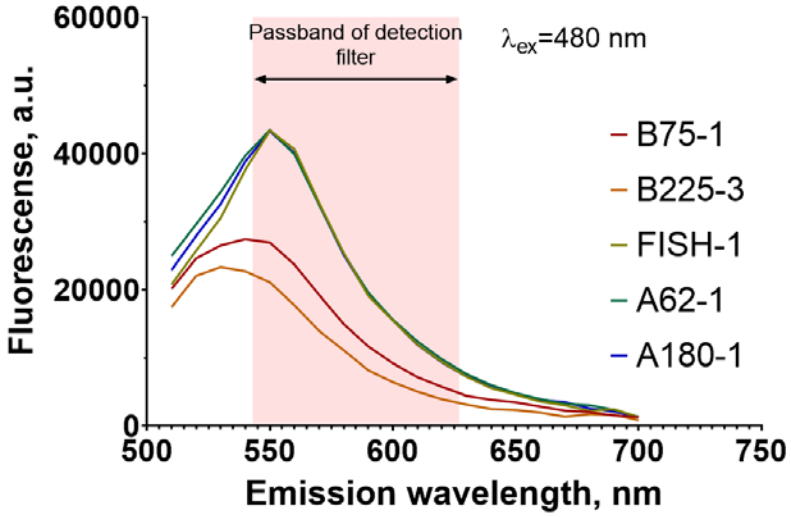

Figure S4. Fluorescence intensity of gelatin nanoparticles in the passband of detection filter

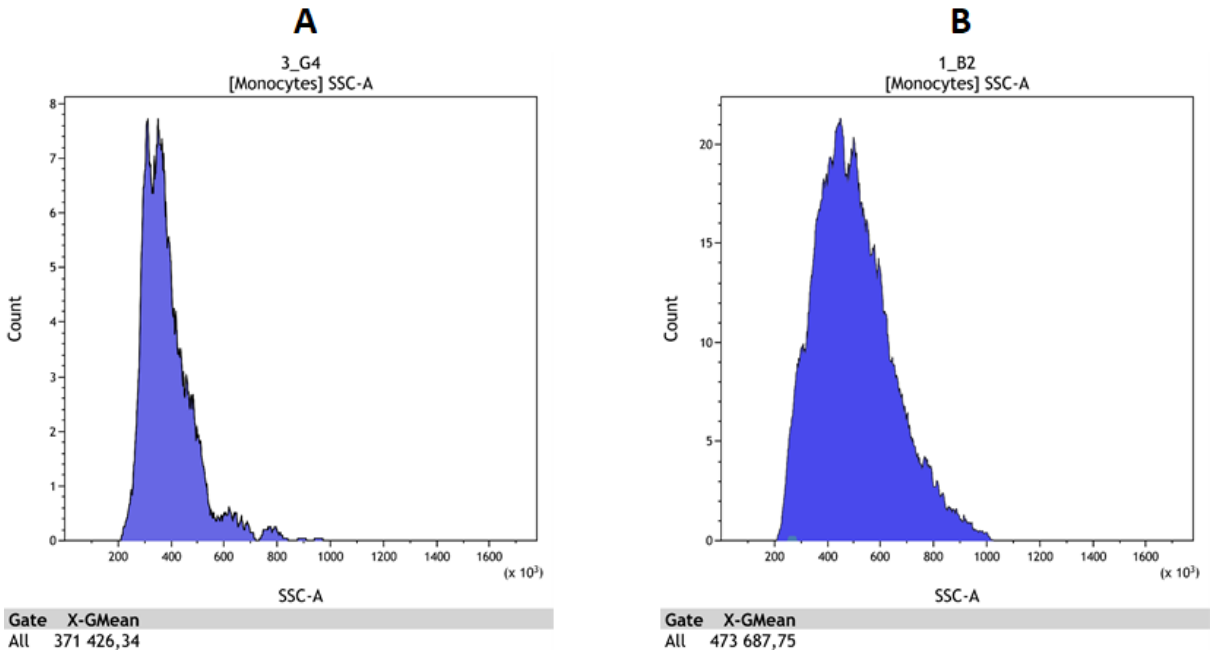

Figure S5. SSC histograms of monocyte gate in negative control without particles with water (A) and in the sample with 1000 µg/mL of particles (B). The geometric means of SSC intensities are indicated below the histograms.

Table S1. Yields of gelatin nanoparticles prepared by various methods

No.	Method	Yield	Gelatin	Size	Reference
1	One-step desolvation	69-83% (standard batch size) 70% (scaled batch size)	High-bloom (300) gelatins A and B	150-300 nm	(**Geh, 2016**)
2	Two-step desolvation	1.5%	Gelatin type A 300 bloom	-	(**Geh, 2016**)
3	Nanoprecipitation	39-82%	Gelatin with bloom numbers from 75 to 300.	Paclitaxel-loaded nanoparticles 600-1000 nm	(**Lu, 2004**)
4	Nanoprecipitation	90±5%	Gelatin type A 250 bloom	Doxorubicin-loaded gelatin nanoparticles, 100-200 nm	(**Leo, 1997**)
5	Two-step desolvation	70-75%	Gelatin type A 175 bloom	Antibody-labelled nanoparticles, 250-300 nm (PdI= 0.02)	(**Balthasar, 2005**)
6	Nanoprecipitation	73%	Gelatin type was not specified	191 nm	(**Das, 2020**)
7	Nanoprecipitation	20-34%	Gelatin B 75 bloom	200-300 nm	(**Khan, 2015**)

8	Nanoprecipitation	23%	Gelatin B 75 bloom	200-300 nm	(**Lee, 2011**)
9	Two-step desolvation	less than 30%	Gelatin type A 175 bloom	140-200 nm	(**Fuchs, 2010**)
10	Two-step desolvation	26-51%	Gelatin type A 175 bloom	100-300 nm	**Zwiorek, 2006**
11	One-step desolvation (high molecular weight fractions were desolvated)	up to 62%	Gelatin type A, bloom value is not specified	50-260 nm	**Shamarekh, 2020**